

DTIC FILE COPY

AD-A202 621



01 DTIC

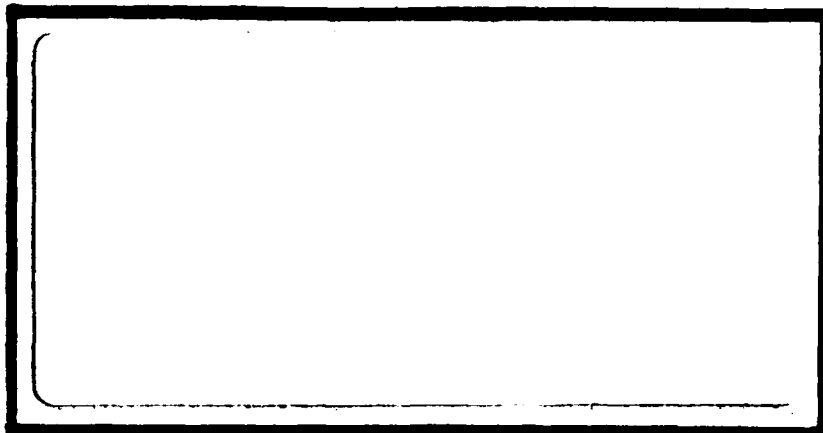
ELECTED

JAN 18 1980

S

D

0 H



DEPARTMENT OF THE AIR FORCE

• AIR UNIVERSITY

**AIR FORCE INSTITUTE OF TECHNOLOGY**

Wright-Patterson Air Force Base, Ohio

DISTRIBUTION STATEMENT A

Approved for public release;  
Distribution Unlimited

89 1 17 003

AFIT/GSO/ENP/88D-2

SPACECRAFT CHARGE AS A SOURCE  
OF ELECTRICAL POWER FOR SPACECRAFT  
THESIS

Wayne Gale  
Flight Lieutenant, RAAF

AFIT/GSO/ENP/88D-2

Approved for public release; distribution unlimited.

AFIT/GSO/ENP/88D-2

SPACECRAFT CHARGE AS A SOURCE  
OF ELECTRICAL POWER FOR SPACECRAFT

THESIS

Presented to the Faculty of the School of Engineering  
of the Air Force Institute of Technology  
Air University  
In Partial Fulfillment of the  
Requirements for the Degree of  
Master of Science in Space Operations

Wayne Gale, B.E.  
Flight Lieutenant, RAAF

November 1988

Approved for public release; distribution unlimited

### Preface

Spacecraft charging has been under investigation for a number of years to gain an understanding of the processes involved, and to design spacecraft and materials to eliminate or limit charge buildup. The purpose of this study, however, was to determine if the charge that collects on spacecraft is sufficient to provide a useful source of power for spacecraft. An analytical solution approximation was selected here to obtain order-of-magnitude charging calculations. The research showed that the energy available from the surface charge is limited; therefore, continued efforts to eliminate charging appears to be the best option.

I am indebted to Henry B. Garrett for his 1981 review of spacecraft charging. This paper filled many of the gaps in my knowledge on the history of spacecraft charging and the approaches taken to modelling charging mechanisms. I wish to thank my thesis advisor LtCol H. E. Evans for his assistance and patience during my research. To my friends, Maj Bob Chekan and Capt Alan Sterns, many thanks for your ideas and encouragement during our thesis discussions. Finally, I wish to thank my wife Margaret for her assistance in editing and her limitless patience during my involvement with this work.

Wayne Gale

Table of Contents

|  | <u>Page</u> |
|--|-------------|
| Preface . . . . .                                    | ii          |
| List of Figures . . . . .                            | v           |
| List of Tables . . . . .                             | vii         |
| Notation . . . . .                                   | viii        |
| Abstract . . . . .                                   | xi          |
| I. Introduction . . . . .                            | 1.1         |
| General Background . . . . .                         | 1.3         |
| Problem Statement and Research                       |             |
| Questions . . . . .                                  | 1.6         |
| Limitations and Assumptions . . . . .                | 1.7         |
| Basic Approach . . . . .                             | 1.8         |
| II. Literature Review . . . . .                      | 2.1         |
| Background Physics . . . . .                         | 2.1         |
| Plasma . . . . .                                     | 2.1         |
| Charge in Conductors . . . . .                       | 2.4         |
| Surface Charging in Plasma . . . . .                 | 2.5         |
| Plasma Probe Theory . . . . .                        | 2.11        |
| Modelling of Spacecraft Charging Processes . . . . . | 2.13        |
| Plasma Environment Modelling . .                     | 2.16        |
| Plasma Sheath Modelling . . . . .                    | 2.18        |
| Spacecraft Surface and Discharge Modelling . . . . . | 2.20        |
| NASCAP . . . . .                                     | 2.21        |
| Discharge Transient Modelling . .                    | 2.24        |
| Analytical Modelling . . . . .                       | 2.25        |
| III. Methodology . . . . .                           | 3.1         |
| Geosynchronous Plasma Environment . .                | 3.1         |
| Charging Model . . . . .                             | 3.2         |
| Application of the Charging Model . .                | 3.4         |
| IV. Geosynchronous Plasma Environment . . . . .      | 4.1         |

|  | <u>Page</u> |
|--|-------------|
| V. Charging Model . . . . .  | 5.1         |
| Plasma Flux Density . . . . .  | 5.2         |
| Charging Model Current Terms . . . . .   | 5.4         |
| Photoelectron Emission . . . . .   | 5.6         |
| Secondary Electron Emission and<br>Backscatter . . . . .                           | 5.7         |
| Surface Charging Model Development . .   | 5.8         |
| VI. Application of the Charging Model . . . . .                                    | 6.1         |
| Plasma Current density . . . . .   | 6.1         |
| Charging in Sunlit Conditions  |             |
| - Worst Case Plasma . . . . .  | 6.2         |
| Charging in Sunlit Conditions  |             |
| - Average Plasma . . . . .   | 6.13        |
| Eclipse Charging . . . . .   | 6.19        |
| Spacecraft Charge as a Power Source .  | 6.20        |
| VII. Conclusions . . . . .   | 7.1         |
| Limitations . . . . .  | 7.2         |
| Appendix : MATHCAD 2.0 Document for Solving<br>Spacecraft Charging Equations . . . | APP.1       |
| Bibliography . . . . .   | BIB.1       |
| Vita . . . . .   | V.1         |



| Accession For       |                                     |
|---------------------|-------------------------------------|
| NTIS GRA&I          | <input checked="" type="checkbox"/> |
| DTIC TAB            | <input type="checkbox"/>            |
| Unannounced         | <input type="checkbox"/>            |
| Justification       |                                     |
| By _____            |                                     |
| Distribution/ _____ |                                     |
| Availability Codes  |                                     |
| Dist                | Avail and/or<br>Special             |
| A-1                 |                                     |

List of Figures

| <u>Figure</u>   | <u>Page</u> |
|---|-------------|
| 2.1 Surface Potential and Sheath of a Plasma Charged Isolated Surface                                 | 2.7         |
| 2.2 Current Density - Voltage Characteristic of a Plasma Probe  | 2.13        |
| 3.1 Spacecraft Charging Model   | 3.2         |
| 6.1 Sunlit Surface Potential in Worst case Plasma - No Rotation                                       | 6.4         |
| 6.2 Shaded Surface Potential in Worst Case Plasma - No Rotation                                       | 6.5         |
| 6.3 Differential Surface Potential in Worst case Plasma - No Rotation                                 | 6.6         |
| 6.4 Discharge Current Effect on Sunlit Surface Potential in Worst Case Plasma for Rotating Spacecraft | 6.8         |
| 6.5 Discharge Current Effect on Shaded Surface Potential in Worst Case Plasma for Rotating Spacecraft | 6.9         |
| 6.6 Discharge Current Effect on Shaded Surface Potential in Worst Case Plasma for Rotating Spacecraft | 6.10        |
| 6.7 Differential Surface Potential in Worst Case Plasma for Rotating Spacecraft                       | 6.11        |
| 6.8 Differential Surface Potential in Worst Case Plasma for Rotating Spacecraft                       | 6.12        |
| 6.9 Surface Potentials in Average Plasma - No Rotation  | 6.14        |
| 6.10 Differential Surface Potential in Average Plasma - No Rotation                                   | 6.15        |
| 6.11 Sunlit Surface Potential in Average Plasma for Rotating Spacecraft                               | 6.16        |

|  | <u>Page</u> |
|--|-------------|
| 6.12 Shaded Surface Potential in Average Plasma<br>for Rotating Spacecraft                       | 6.17        |
| 6.13 Shaded Surface Potential in Average Plasma<br>for Rotating Spacecraft                       | 6.18        |
| 6.14 Differential Surface Potential in Worst Case<br>Plasma - No Rotation (2 times Surface Area) | 6.22        |

## List of Tables

| <u>Table</u>   | <u>Page</u> |
|--|-------------|
| 4.1 Worst Case Geosynchronous Plasma                                       | 4.2         |
| 4.2 Average Plasma Environment: ATS-5 (1969-1970)                          | 4.3         |
| 5.1 Plasma Current Density at Geosynchronous Altitude                      | 5.4         |
| 5.2 Debye Lengths for Geosynchronous Environment                           | 5.5         |
| 5.3 Secondary Emission and Backscattered Electron Parameters for Aluminium | 5.8         |
| 6.1 Maximum Plasma Current to One Surface of the Spacecraft                | 6.2         |

### Notation

|          |   |   |                |
|----------|---|---|----------------|
| $A$      | = | surface area exposed to incident plasma particles   | ( $m^2$ )      |
| $A_{ph}$ | = | effective surface area exposed to solar radiation   | ( $m^2$ )      |
| $BS_e$   | = | backscattered electrons parameter                   |                |
| $E$      | = | electric field intensity                            | (volt/m)       |
| $f$      | = | distribution function                               |                |
| $F$      | = | fraction of surface area exposed to solar radiation |                |
| $F$      | = | force   | (Newton)       |
| grad     | = | gradient operator                                   |                |
| $i$      | = | particle species                                    |                |
| $I$      | = | current to surface                                  | (amps)         |
| $I_{bs}$ | = | backscattered electron current                      | (amps)         |
| $I_e$    | = | electron current                                    | (amps)         |
| $I_i$    | = | ion current   | (amps)         |
| $I_{ph}$ | = | photoelectron current                               | (amps)         |
| $I_{se}$ | = | secondary electron emission due to electrons        | (amps)         |
| $I_{si}$ | = | secondary electron emission due to ions             | (amps)         |
| $I_t$    | = | total current to spacecraft                         | (amps)         |
| $J$      | = | current density                                     | (amps/ $m^2$ ) |
| $J_e$    | = | electron current density                            | (amps/ $m^2$ ) |
| $J_i$    | = | ion current density                                 | (amps/ $m^2$ ) |
| $J_{ph}$ | = | photoelectron current density                       | (amps/ $m^2$ ) |

|                       |   |                        |
|-----------------------|---|------------------------|
| $J_{pho}$             | total photoelectron current density (normal incidence)            | (amps/m <sup>2</sup> ) |
| $K$                   | Boltzmann Constant  | (j/°K)                 |
| $KE_{av}$             | average kinetic energy  | (joules)               |
| $m$                   | mass of particle  | (kg)                   |
| $m_e$                 | mass of an electron   | (kg)                   |
| $m_i$                 | mass of an ion  | (kg)                   |
| $N$                   | particle number density   | (m <sup>-3</sup> )     |
| $N_e$                 | electron particle density   | (m <sup>-3</sup> )     |
| $N_e'$                | depleted particle density   | (m <sup>-3</sup> )     |
| $N_o$                 | plasma density  | (m <sup>-3</sup> )     |
| $q$                   | electric charge   | (coul)                 |
| $S_e$                 | secondary electron emission parameter - due to incident electrons |                        |
| $S_i$                 | secondary electron emission parameter - due to incident ions      |                        |
| $T$                   | Absolute Temperature  | (°K)                   |
| $T_e$                 | absolute temperature of electrons                                 | (°K)                   |
| $T_i$                 | absolute temperature of ions                                      | (°K)                   |
| $T_{ph}$              | photoelectron temperature   | (°K)                   |
| $v$                   | velocity of particle  | (m/s)                  |
| $V$                   | electric potential  | (volt)                 |
| $\langle v \rangle^2$ | mean square speed   |                        |
| $v_{av}$              | average particle speed  | (m/s)                  |
| $V_s$                 | surface potential   | (volts)                |
| $V_p$                 | plasma potential  | (volts)                |
| $V(r)$                | voltage at distance $r$ from surface                              | (volts)                |

|              |   |  |                        |
|--------------|---|--|------------------------|
| $x$          | = | angle of incidence of solar<br>radiation | (degrees)              |
| $\epsilon_0$ | = | permittivity of free space               | (farad/m)              |
| $\lambda_d$  | = | Debye length                             | (metres)               |
| $\theta$     | = | angle of rotation of spacecraft          | (radians)              |
| $\rho$       | = | surface charge density                   | (coul/m <sup>2</sup> ) |

Abstract

This thesis examines the suitability of spacecraft charge, collected at geosynchronous altitude, as a source of electrical power for spacecraft. An analytical plasma probe model is used to describe the flux of charged particle currents on two isolated (conductive) hemispheres of a spacecraft. Surface potentials are evaluated for both a body-stabilized and spin-stabilized spacecraft under average and worst case plasma conditions. A discharge current is simulated, between differentially charged surfaces, to examine the current flow required to balance the surface potentials. This current approximates the maximum current flow available from the spacecraft charge. The results show that surface potential differences can be large in worst case plasma conditions, but the current available is too small to be useful as a power source. The discharge current does scale up in proportion to spacecraft surface area exposed to the plasma; however, the design of large conductive spacecraft surfaces is a problem in itself.

SPACECRAFT CHARGE AS A SOURCE OF  
ELECTRICAL POWER FOR SPACECRAFT

I. Introduction

Spacecraft charge is a static electric charge which collects on the external surfaces of spacecraft. The charge may not develop uniformly over a spacecraft surface because of the dynamic nature of the interaction of spacecraft surface materials with the surrounding space environment. The subsequent electrical potential difference developed between separated surfaces can cause electrical arcing problems if the potential exceeds the breakdown voltage of the insulation. However, the potential difference may be useful if it can force an electrical current through a circuit inside the spacecraft and provide some electrical power for the spacecraft.

In the early 1970's a number of geosynchronous satellite programs were reporting spurious switching activity near the local midnight region of the satellite orbits (Lovell and others, 1976:3-14). Investigations into

the problem showed that charged particle fluxes with higher than expected energies, in the region around the satellites, were causing the satellite system interruptions. The high energy particle fluxes were interacting with the satellite surfaces causing them to become charged. The resulting surface potentials were reaching levels sufficient to cause arc discharges between insulated satellite surfaces. Electronic equipment in the spacecraft was being disrupted by the pulse of discharge current which coupled into the spacecraft electrical cabling and electronic equipment.

Research into spacecraft charging has continued in some depth since the early 1970's with a joint technology program between the USAF and NASA. The objective of the investigation has been to provide the design criteria, materials, techniques, and test methods to ensure control of the charging processes on spacecraft surfaces. The work involved modelling and simulation of the environment, spacecraft surface materials development to control charging, flight experiments to test the developments, and also updating spacecraft design criteria and test specifications. The initial program was planned for four years, from July 1975 to October 1979, to include data analysis from the ATS-5 (Advanced Technology Satellite), ATS-6, and SCATHA (Spacecraft Charging at High Altitude)

flight test satellites. As a result of this research, NASA was able to issue guidelines for designers to use in assessing and controlling spacecraft charging effects (Purvis and others, 1984:1-36).

The previous research into spacecraft charging has therefore concentrated on understanding the phenomenon and developing methods to control or eliminate the charging. This thesis, however, investigates the possible use of spacecraft charge as a source of electrical energy. The added benefit of using spacecraft charge would be to provide an automatic charge control mechanism.

#### General Background

Spacecraft charging results mainly from the interaction of spacecraft surfaces with the following:

- a. charged particle flux in the surrounding space plasma,
- b. photoelectrons caused by incident solar radiation,
- c. electron emission caused by incident high energy electrons and ions, and
- d. incident high energy cosmic particles penetrating the spacecraft surface.

These lead to the following two basic modes in which spacecraft can charge:

1. absolute, and
2. differential charging.

Absolute charging occurs when an entire spacecraft surface charges to a potential relative to the surrounding plasma (but absolute charging is not the main cause of problems).

Differential charging occurs when parts of a spacecraft charge to different potentials, and has been known to cause disruption and damage to spacecraft surfaces and equipment.

The combination of charging processes and modes determine the resultant electrical surface potential and charge distribution. The particle fluxes are dynamic in nature, and, when interacting with satellites that have typically irregular geometries and surface materials, the potential distribution around a satellite may be highly asymmetric.

A generally recognized simplification is that, at altitudes above about three earth radii, the ambient plasma environment is thin and the photoelectron current emitted by solar irradiated satellite surfaces will dominate the electron flux from the plasma (McPherson and Schröber 1976:15-21). This will result in a positive charge on the

illuminated satellite surface with respect to the plasma environment. At lower altitudes however, where the plasma is more dense (less than three earth radii) the plasma currents will dominate the photoelectron currents and the satellite will tend to become more negative than the plasma. For either altitude case there is a production of photoelectrons on the illuminated side of the satellite so the flux of charged particles around the satellite will change continuously to maintain equilibrium. (The flow of currents and charge distribution is also complicated by factors such as satellite spin and earth eclipse conditions.)

Differential charging can generate significant electric fields between insulated spacecraft surfaces. Electrical arc discharges will occur if the insulation breakdown potential is exceeded. Subsequent arc discharges may cause damage to the spacecraft. The thermal properties of satellite surfaces may also be damaged and cause an increase in the operating temperature of internal components. The higher operating temperatures may reduce satellite lifetime. Furthermore, an arc discharge generates electromagnetic energy which can couple into electric cables and disrupt or damage electrical equipment (Lovell and others, 1976:4-5).

Discharges may also cause long-term degradation of surface coatings and increased surface contamination.

Problem Statement and Research Questions

Research and analysis are thus required to determine if spacecraft charge developed at geosynchronous orbit can be collected and utilized as a power source for spacecraft. The following is then a list of significant research questions which each need to be answered in order to evaluate a spacecraft charge collection system as a viable source of energy for spacecraft:

1. Can the spacecraft environmental processes at geosynchronous orbit be characterized for prediction of spacecraft surface charging effects? (Chapter IV)
2. Can the spacecraft surface interaction currents be modelled for computation of the charging effects? (Chapter V)
3. What is the time scale involved in the development of spacecraft charge? (Chapter V)
4. How much surface charge is developed on a conductive satellite in geosynchronous orbit? (Chapter VI)
5. What effect does spacecraft spin and position in orbit have on the development of spacecraft charge? (Chapter VI)
6. How much electrical power can be drawn from the surface of a spacecraft for use as a source of power? (Chapter VI)

7. How useful will a spacecraft charge collection be as a means of providing power for spacecraft in the future?  
(Chapter VI)

Limitations and Assumptions

Extensive research has already been initiated into the complex phenomenon of spacecraft charging. The research proposed here will utilize the existing knowledge of charging processes at geosynchronous orbit to determine if the electrical energy collected on spacecraft surfaces can be useful as a source of power. The following limitations and assumptions will be made to narrow the field of research:

- a. Environmental processes will only be investigated for background knowledge on geosynchronous plasma processes and to specify plasma conditions for input to a charging model.
- b. A charge collection method will be proposed to enable predictions of the amount of electrical current that may be available from a charged spacecraft.  
Integration of the charge collector into an actual spacecraft system will not be examined.

- c. A cost analysis for the implementation of a charge collection system will not be examined.
- d. The spacecraft charging process model selected from a review of the literature will be adopted for use here without in depth validation.
- e. A simplified spherical spacecraft structure with two isolated hemispheres of conductive surface material will be used as a surface charging model.

#### Basic Approach

The basic approach to this research is as follows:

- a. determine charging environmental conditions at geosynchronous altitude;
- b. obtain a suitable model of spacecraft surface charging processes;
- c. evaluate surface charging and the electrical potentials developed on the surfaces of a spacecraft structure;
- d. evaluate the possibility and amount of electrical power that can be drawn from the spacecraft surface; and

e. make recommendations for the suitability  
of a spacecraft charge collection system  
in future spacecraft.

## II. LITERATURE REVIEW

The research material examined here includes the principles of static electricity, plasma physics, and existing knowledge of spacecraft charging. This review is separated into the following two topic areas:

- a. background physics, and
- b. modelling of spacecraft charging processes.

### Background Physics

Static charge collected on the surfaces of spacecraft in orbit causes an electric potential to develop on the surfaces which produces electric fields in the surrounding space. The background presented here describes the interaction processes between conductive spacecraft surfaces and the surrounding plasma. Classical static electricity principles are introduced from Tamm (Tamm, 1979:23-107). Conceptual and mathematical relationships are included to describe the charging effects on a conductor surface in plasma. Plasma probe theory is also introduced because it was used to develop initial spacecraft charging models.

Plasma. Chapman describes a plasma as a partially ionized gas (typically 0.01% ionized) with equal numbers of

positive and negative charges, so plasma has an overall neutral charge (Chapman, 1980:49). Most plasma particles are un-ionized neutral particles so the interaction between charged particles is infrequent. Only charged particles are significant in charging processes so the plasma discussed here refers to the charged particles within the plasma.

Charge concentrations do not tend to exist in a plasma because the overall charge is balanced; however, when plasma is disturbed by an external electric field the charge balance can be disturbed. Chen describes a collective behaviour characteristic to plasma in which a collection of charge at one region in a plasma can cause strong electrostatic forces which may affect plasma motion over a substantial distance in the plasma (Chen, 1974:3-4).

Plasma can be characterized by charged particle energy and density. The average kinetic energy of a particle depends on particle speed and mass, and is often expressed in terms of the absolute temperature of the gas particles. Eqs (2.1) and (2.2) give the relationship between kinetic energy, mass, velocity, and temperature of a gas particle. Eq (2.1) is derived from the isotropic Maxwell-Boltzmann distribution function in Eq (2.3) which describes the velocity distribution of a gas (species i) for a given

absolute temperature. This distribution is used here to define a plasma.

$$KE_{av} = (m\langle v \rangle^2)/2 \quad (2.1)$$

$$KE_{av} = (3/2)KT \quad (2.2)$$

$$f(v) = N_i (2/\pi)^{0.5} (m_i/2KT_i)^{1.5} v^2 \exp(-m_i v^2/(2KT_i)) \quad (2.3)$$

where

$KE_{av}$  = average kinetic energy (joules)

$m$  = mass of particle (kg)

$v$  = velocity of particle (m/s)

$K$  = Boltzmann Constant (j/°K)

$T$  = Absolute Temperature (°K)

$i$  = particle species

$f$  = distribution function

$\langle v \rangle^2$  = mean square speed

$N$  = particle number density ( $m^{-3}$ )

The average speed of the gas particles, given by Eq (2.4), shows the inverse relationship between the speed and mass of a particle.

$$v_{av} = (8KT/\pi m)^{0.5} \quad (2.4)$$

where

$v_{av}$  = average speed (m/s)

This implies that electrons in a plasma have a higher average speed than ions because the mass of an electron is about 1800 times less than that of an ion (assuming an ion has the mass of a proton). For a typical plasma temperature at geosynchronous altitude of about 1 eV (electron volt), or  $11500^{\circ}\text{K}$ , this gives an electron speed of about  $6.7 \times 10^5$  m/s which is to be compared with spacecraft orbital speed of  $3 \times 10^3$  m/s. So geosynchronous spacecraft are relatively stationary with respect to the plasma environment.

Charge in Conductors. Charge flow equilibrium implies no overall flow of charged particles. The static charge collected on a conductor can be shown by Gauss's Law to only distribute on the surface of the conductor. This surface charge generates an electric field in the region around the surface. Charged particle fluxes to an isolated conductor in plasma redistribute in about  $10^{-3}$  seconds (Katz and others, 1977:320). Therefore, the charging time of a conductor can be considered as static with respect to geosynchronous plasma environment changes, which typically occur on a time scale from seconds to hours.

The electric field intensity  $\mathbf{E}$ , resulting from a surface charge, is a vector quantity normal to the surface at every point on the surface. Consequently, the  $\mathbf{E}$  field

close to the surface can be given by Eq (2.5) and is only dependent on the surface charge density at that point on the surface and not on the distribution of charge at other places in the field.

$$E = \rho/\epsilon_0 \quad (2.5)$$

where

$E$  = electric field intensity (volt/m)

$\rho$  = surface charge density (coul/m<sup>2</sup>)

$\epsilon_0$  = permittivity of free space (farad/m)

Surface Charging in Plasma. Charged plasma particles incident on an isolated conductive surface will result in surface charging and the development of a surface potential. The surface potential increases to balance the charged particle fluxes at the surface. An electric field is established in the space surrounding the charged surface which can affect the local charged particle density. A potential barrier is formed in the region around the charged surface by charged particles that are attracted to the surface. This barrier or shielding effect is the response identified by Chen as one that is characteristic to a plasma environment.

The particle flux incident on a surface in plasma is dependent on the speed and density of the particles in the plasma (Chapman, 1980:51-53). The flux density relationship of plasma to a surface is given in Eq (2.6) for the one-dimensional case. The higher average speed of electrons (as shown in Eq (2.4)) will cause the current density due to electrons to be significantly higher than for ions.

$$J = qNV_{av} \quad (2.6)$$

where

$$\begin{aligned} J &= \text{current density} & (\text{amps/m}^2) \\ q &= \text{electric charge} & (\text{coul}) \end{aligned}$$

This imbalance in current causes a negative charge to develop on the conductive surface. The surface potential increases accordingly and will repel the incident electrons and attract the ions. The surface potential will stabilize when a balance in the electron and ion current density occurs.

The influence of the surface potential extends for some distance from the surface into the plasma. The range of influence of the plasma sheath is determined by the energy and density of the plasma particles in the surrounding plasma. Particles require in excess of a particular energy

level to overcome the space potential barrier, and density determines the mean free path of the particles. Plasma electrons with sufficient energy will arrive at the surface of a negatively charged conductor. Fig 2.1 illustrates the effect of a surface potential, caused by plasma charging, on plasma particles in the region of the charged surface. The plasma sheath due to the negative surface potential is also shown in this figure.

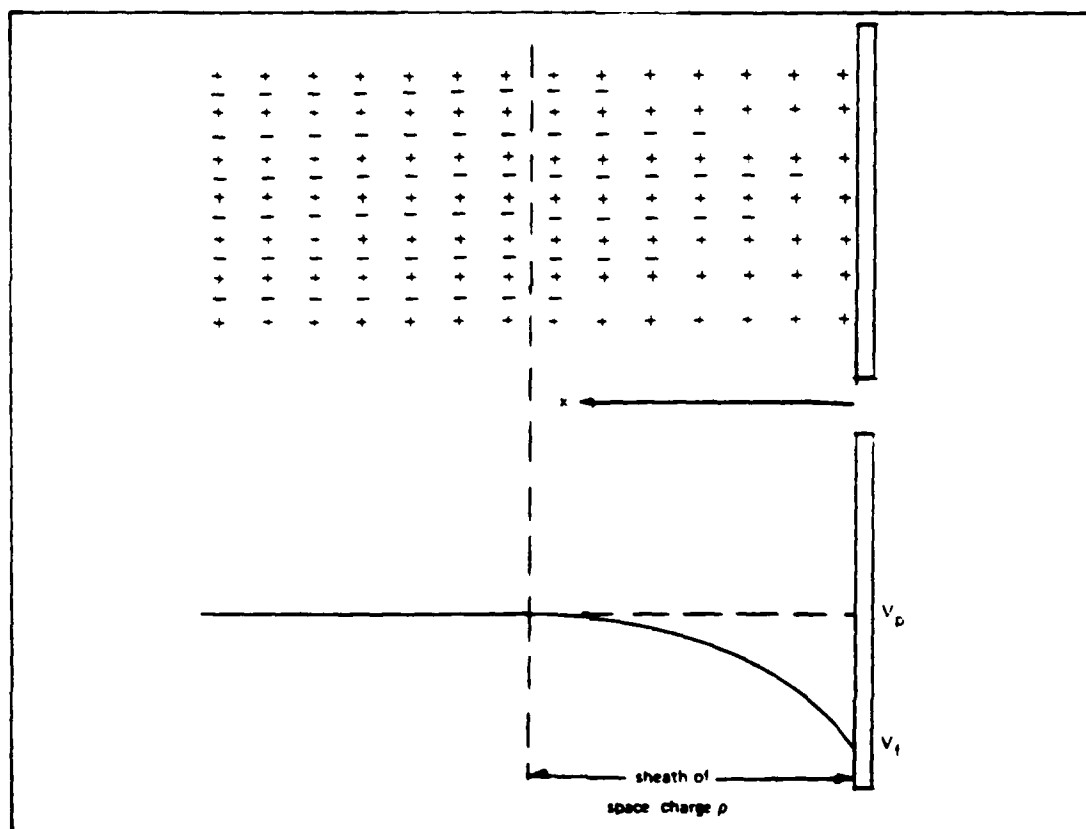


Fig 2.1 Surface Potential and Sheath of a Plasma Charged Isolated Surface

Reproduced from (Chapman, 1980:55)

The electric field in the space around the charged surface will apply a force, given by Eq (2.7), to charged particles in the space. The energy required by electrons to overcome the repulsive force of the electric field is determined from the product of the force and distance. The potential difference between two points in an electric field is defined as the work done by the field in moving a unit positive charge between the two points. Eq (2.8) gives the electric field intensity  $\underline{E}$  at any point in space around a charged surface with potential  $V$ .

$$\underline{F} = q\underline{E} \quad (2.7)$$

$$\underline{E} = -\text{grad } V \quad (2.8)$$

where

$\underline{F}$  = force (Newtons)

$\text{grad}$  = gradient operator

$V$  = electric potential (volt)

The charged particle species depleted in the space around a charged surface has the same polarity as the surface charge (Chapman, 1980:55). The electron density causing the sheath effect around a negatively charged surface can be approximated from Eq (2.9). This equation is obtained from the Maxwell Boltzmann distribution function given in Eq (2.2). Eq (2.9) indicates that electrons are

depleted in the sheath region which gives the sheath an overall positive charge. Electrons that are able to reach the surface require a kinetic energy greater than  $q(V_p - V_f)$ . Chapman develops an approximation in Eq (2.10) for the potential difference across the potential sheath for the Maxwellian particle distribution.

$$N_e' / N_e = \exp[q(V_p - V_f) / K T_e] \quad (2.9)$$

$$V_p - V_f = (K T_e / 2q) \ln(m_i T_e / m_e T_i) \quad (2.10)$$

where

$N_e'$  = particle density in depleted region ( $m^{-3}$ )

$N_e$  = initial particle density ( $m^{-3}$ )

$V_p$  = plasma potential (volts)

$V_f$  = surface potential (volts)

$T_e$  = absolute temperature of electrons ( $^0K$ )

$T_i$  = absolute temperature of ions ( $^0K$ )

$m_i$  = mass of an ion (kg)

$m_e$  = mass of an electron (kg)

Chapman derives Eq (2.11) from Eq (2.10) to define an approximate distance of influence that the charged surface has in the surrounding plasma. This distance is called the Debye length. The Debye length indicates how a potential disturbance is attenuated in the plasma as a function of

distance: for a distance  $\lambda_d$  the perturbation is reduced to 0.37 (1/exp) of the initial value.

$$\lambda_d = (\epsilon_0 K T / q^2 N_0)^{0.5} \quad (2.11)$$

where

$\lambda_d$  = Debye length (m)

$N_0$  = plasma density ( $\text{m}^{-3}$ )

The collective nature of plasma is highlighted by this Debye length attenuation property. This means that charged particles collect around an area of charge concentration and screen voltage perturbations by forming a sheath around the charge. The plasma outside the range of about three Debye lengths is relatively undisturbed by a perturbation at the charged surface.

The relationship between the space charge density and the electric field potential  $V$  as a function of distance from a charged surface is given by Eq (2.12) which is called Poisson's equation.

$$\text{div grad } V = -\rho/\epsilon_0 \quad (2.12)$$

The continuity of plasma particle flow can be expressed by Eq (2.13) which is called the Vlasov equation (Nicholson,

1983:70-73). This equation describes the motion of a plasma with particle distribution  $f_i$  by using the assumptions of time independence, collisionless plasma, and no magnetic field effects. These assumptions have been generally accepted as valid for spacecraft charging at geosynchronous altitude (Garrett, 1981:599-600).

$$\mathbf{v} \cdot \nabla f_i - (q/m_i) \nabla V(r) \cdot \nabla_v f_i = 0 \quad (2.13)$$

where

$i$  = particle species

$f$  = Maxwell-Boltzmann distribution function

$V(r)$  = voltage at distance  $r$  from surface

Eqs (2.12) and (2.13) require treatment in a self-consistent way to solve for the surface potential of a surface in plasma (Garrett, 1981:592,599-600). The surface potential resulting from the charging of a surface will affect the charge density in the region around the charged surface. The space charge density will in turn affect the surface potential. Hence, to solve for the surface potential and charge density, a self-consistent solution technique is required.

Plasma Probe Theory. The plasma theory reviewed up to this point forms the basis for a study of plasma probe

theory. A plasma probe is generally used for plasma measurements and probe dimensions are selected so that the probe causes minimal disruption to the plasma. In the spacecraft charging situation, however, the entire spacecraft is considered to be a probe in plasma. For spacecraft charging there are two significant cases in the application of plasma probe theory. These cases occur when the spacecraft size is either large or small compared to the Debye length (given in Eq (2.11)). Garrett reviews the application of probe theory in the development of spacecraft charging models (Garrett, 1981:592-602). General and specific spacecraft charging models are discussed in the next section of this chapter.

Chapman describes the characteristics of a plasma probe, illustrated in Fig 2.2, in terms of the current density to a probe versus the voltage on the probe (Chapman, 1980:60-70). The net current density is the sum of electron and ion currents. A probe current density characteristic curve can be described by varying the bias potential on a probe. The extremes of this characteristic are either electron or ion saturation conditions. A natural balance of electron and ion current is achieved when the probe surface charges to repel the excess charged particle species from the probe surface. For a spacecraft the current

characteristic is expected to be similar in form. Plasma conditions such as particle density and energy at geosynchronous altitude will dictate the charging levels.

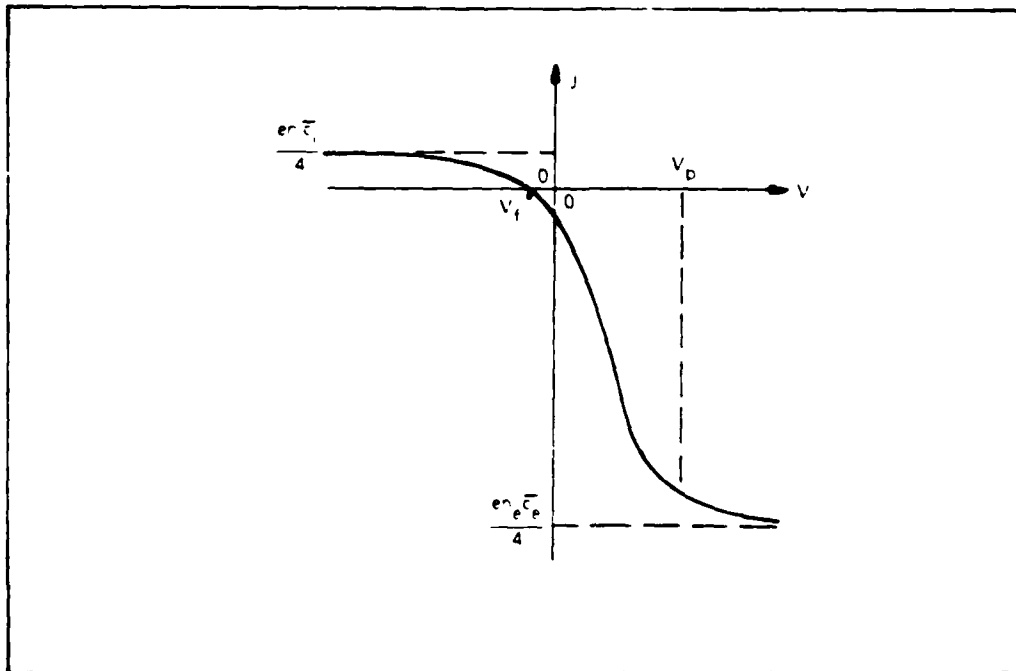


Fig 2.2 Current Density - Voltage Characteristic of a Plasma Probe

Reproduced from (Chapman, 1980:61)

#### Modelling of Spacecraft Charging Processes

This section is organized into a general discussion of spacecraft charging and model requirements, and then a topic by topic discussion of existing models of charging processes. Modelling of spacecraft charging processes is necessary to ensure that spacecraft design concepts and possible problem areas are evaluated before implementation

of the design occurs. Models must be able to reasonably predict losses in spacecraft performance from interaction of a spacecraft with the plasma environment. Charging models will allow the interaction between the external environment and spacecraft equipment to be computed and studied.

Spacecraft charge modelling was originally separated into the following four regions (Whipple, 1977:231):

- a. undisturbed plasma environment,
- b. plasma sheath,
- c. spacecraft surface, and
- d. spacecraft equivalent circuit model.

These regions were adequate for initial study; however, the requirement existed for a more complete analysis which integrated all these model regions. This integration has been done using both analytical and numerical techniques based on plasma probe theory.

Spacecraft performance degradation can occur in the following forms:

- a. Interruption to system operation due to spurious electromagnetic switching events from arc discharge coupling into electrical cables and equipment.

- b. Surface material degradation from arc discharge damage or attraction of unwanted particles by the spacecraft surface charge.

Switching anomalies initially attracted the attention of researchers; however, surface material degradation was also recognized as a significant factor for long term spacecraft operations. Surface degradation may affect the performance of solar cells which are likely to be the primary source of power for long term space flights (O'Donnell, 1978:797).

Spacecraft surfaces are constructed of various materials including mainly conductor and dielectric materials. The response of all these materials to plasma flux and charging must be specified in a complete charging model. The electrostatic discharge coupling processes that occur between the surface materials, the spacecraft structure, and the electrical system must also be modelled.

Analytic techniques were developed using plasma probe theory to examine the interaction of a spacecraft surface structure with the plasma environment. Order of magnitude calculations can be made using simplified relationships and spacecraft geometries; however, numerical simulation methods

are necessary to handle the complex spacecraft structures in real design situations (Garrett, 1981:599-604).

Plasma Environment Modelling. The geosynchronous environment is a space plasma that can be characterized by particle temperature and density for each particle species. This plasma can be significantly affected by the flux of particles from outside the plasma. Solar wind fluctuations cause geomagnetic substorm activity, which can inject high energy particle clouds into the plasma. Geosynchronous spacecraft can encounter both undisturbed and disturbed plasma, and significant charging may occur when spacecraft enter these clouds of high energy plasma particles.

Modelling of the geosynchronous environment is difficult due to the dynamic nature of the external solar and cosmic influences. At least four magnetospheric models types are in common use by spacecraft charging investigators (Garrett, 1978:11-17). The models are broadly classified as follows:

- a. statistical;
- b. analytical;
- c. static field; and
- d. complex, three dimensional, real time simulators.

Only the statistical and analytical models are discussed here, but Garrett also cites work done with other model types.

Statistical models have been derived from average plasma particle energy and flux distributions for various altitudes and locations in the magnetosphere. A statistical model for the magnetosphere has been produced from data collected by the ATS-5 and ATS-6 satellites. The statistical functions were computed using satellite experiment data measurements of solar wind, plasma particle energy, and density. One main limitation of statistical models is the inability to simulate plasma changes over time. However, average parameter values and their ranges are useful for prediction purposes.

An analytical model was also developed from the ATS-5 and ATS-6 statistical data model to satisfy the time response element lacking in the statistical model (Garrett, 1978:15-17). Regression techniques were used to relate satellite data to the time of event occurrence. The time period selected was from local midnight to dawn where the maximum number of spacecraft charging events are known to occur (McPherson and Schrober, 1976:17-18). This analytical model developed for the USAF Geophysics Laboratory (AFGL)

has known biases for charging predictions, when used during daylight hours, but the predictions are sound from midnight to dawn where plasma flux changes are most significant.

Garrett also reports on research by AFGL to determine if the single Maxwellian plasma representation is valid for a geosynchronous plasma (Garrett, 1978:17). Statistical derivations of absolute plasma temperature parameters did not verify the single Maxwellian assumption. A two Maxwellian particle distribution is recommended for use as a minimal plasma representation.

NASA has compiled plasma data from a number of experimental satellite programs for describing a typical geosynchronous plasma environment (Purvis and others, 1984:3,26-30). This data is specified for use as a guide for assessing maximum charging on a spacecraft. Values are given in statistical terms with average and standard deviations for electrons and ions. A summary of worst case environment values is also given for the maximum charging case.

Plasma Sheath Modelling. A spacecraft plasma sheath is the electrical potential barrier formed around a spacecraft caused by charged particle depletion near a charged surface.

Sheath formation depends on spacecraft surface exposure to solar irradiation and plasma particles. Laframboise presents a two dimensional spacecraft charging model called CYLVIA (Cylinder Voltages in the Ionosphere and Above) which accounts for plasma sheath effects (LaFramboise and others, 1980:709-716).

Photoelectrons are emitted by sunlit surfaces and cause a different charging balance than for shadowed surface charging. On shadowed surfaces the plasma dominates charging and a negative potential results (the probe in plasma case). Photoelectron emission results in a positive charge on the emitting surface. The plasma sheath boundary size depends on the equilibrium surface potential. Measurements on the ATS-5 satellite show that the plasma sheath could extend out to 400 metres from a satellite surface (McPherson, 1976:18-19). This large sheath size results from the eclipsed surface charging from a high energy, low density plasma. An irradiated surface will tend to suppress this sheath by the emission of electrons. Therefore, the plasma sheath is likely to vary significantly with solar irradiation.

CYLVIA computes spacecraft surface current density and surface potentials as a result of plasma and photoelectron

flux. The model accounts for the plasma sheath boundary effects by using particle orbit equations to compute current density in two distinct regions. One region reaches from the spacecraft surface where photoelectrons originate out to the sheath boundary. The other region is outside the plasma sheath boundary. Photoelectrons with sufficient energy will cross this boundary. Laframboise identifies earlier models that failed to explicitly account for the sheath boundary, and shows that omission of the sheath boundary causes significant errors in particle current density computations.

#### Spacecraft Surface and Discharge Modelling.

Researchers have investigated spacecraft surface charging interactions in depth and specific models have been generated for studying arc discharge events, coupling of discharges into internal electrical circuits, and spacecraft materials damage (O'Donnell, 1978:798-780). One charging model called NASCAP (NASA Charging Analyzer Program) is discussed here because it is in use as a design validation tool for spacecraft systems. The design guidelines issued by NASA for assessing and controlling spacecraft charging cite NASCAP as an essential tool for charging evaluation (Purvis and others, 1984:5-10).

NASCAP. NASCAP is a computer program developed to model spacecraft charging at high altitudes. The program has been validated with flight data and has predicted charging process interactions to within 10% accuracy (Katz and others, 1978:105-106). NASCAP can model charging of complex spacecraft surface structures by using the following characteristics:

- a. a three dimensional grid surface representation of a spacecraft and the surrounding space;
- b. independent spacecraft surface material specifications;
- c. Sunlight exposure on specific surface elements; and
- d. time dependent development of surface charging processes.

Graphical plots of static charge and surface potential can be produced. Flux breakdown printouts show where surface material breakdown potentials have been exceeded for individual surface elements.

Stannard discusses the validation of NASCAP using data from the SCATHA satellite that was launched in 1979 (Stannard, 1982:1-12). SCATHA was specifically designed to test spacecraft charging processes at geosynchronous orbit.

A grid model of the satellite was constructed in NASCAP which included the same surface material characteristics as SCATHA.

Simulations were run to compare NASCAP predictions with actual measurements from the SCATHA satellite data. NASCAP predicted the gradual development of a negative charge on the shadowed surfaces of SCATHA, and the eventual dominance of the charge on the whole satellite. The final distribution was an overall negative potential, but with the sunlit side positively charged with respect to the eclipsed surfaces (a result of the photoelectron emission). For example, in one run the final eclipsed surface potential was predicted to be -22 Volts, but -100 Volts was actually measured. Stannard considers that faithful prediction of the charge collection process is more important than the actual voltage measured at these small voltage levels. NASA charging guidelines confirm that charge differentials of less than 500 Volts should not cause any electrostatic discharge problems (Purvis and others, 1984:3).

Stannard found that NASCAP was able to accurately predict the dominance of photoelectron current over plasma current at geosynchronous orbit, and the differential charging between insulated surfaces. However, the eclipse

charging simulation was unable to accurately predict short term magnetic sub-storm effects due to the coarse time interval used for the simulation. Fluctuations of up to 4000 volts were measured over periods of less than 20 seconds (NASCAP was using a time interval of 40 seconds).

Surface charging simulation for specific SCATHA surface materials produced accurate estimates compared to the equilibrium potentials measured; however, the dynamic simulation behaviour did not correspond with real data. Sanders also identifies a concern in the accuracy of NASCAP for voltage stress analysis (Sanders and Inouye, 1980:389). The computer model surface element size may not be small enough to accurately resolve the stress potentials at surface edges.

Secondary electron emission effects are also included in the NASCAP model because past experimental research has shown that the ratio of secondary electrons to incident electrons is a significant factor in overall spacecraft charging (Katz and others, 1987:14-1). Secondary electrons are generated by high energy electrons incident on spacecraft surfaces. These secondary electrons typically have low energies, in the order of one electron volt, and are easily influenced by weak electric fields. The electric

fields resulting from a charge on one section of a spacecraft can suppress secondary electron emission on another section of the spacecraft. Therefore, an overall surface charging effect can occur despite the dominance of secondary electrons over incident electrons. Electric fields can also transport secondary electrons between insulated surfaces which increases the effective charging area (Katz and others, 1987:14-3).

The NASCAP program has been validated for use in the engineering of spacecraft systems at geosynchronous orbits (Bass and others, 1986:1). Bass describes how the NASCAP program can be utilized through the SPAN (Space Physics Analysis Network) computer system which is connected to many scientific, defence, and educational institutes in the USA. The program can provide graphical plots via the SPAN, or allow data to be downloaded for use elsewhere. A user's manual is also available to assist in developing appropriate spacecraft models for execution on NASCAP (Cassidy, 1978:1-200).

Discharge Transient Modelling. Modelling of discharge transients and coupling of energy into spacecraft is necessary to determine how susceptible spacecraft systems are to electromagnetic interference. The SCREENS

(Spacecraft Response to Environments of Space) technique uses NASCAP to generate spacecraft surface potentials and charge distributions, and then allows the charge to be coupled into an equivalent circuit model of the spacecraft under test (Stevens and others, 1987:257-263). The model output is used as transient pulse input to another simulation which predicts the response of the electronic equipment under test to an arc discharge.

SCREENS uses a basic rule to determine how much energy is coupled from the discharge site into the cable system. The energy transferred is approximately proportional to the square root of the surface area of the discharge surface (Stettner and others, 1980:1784). A short duration discharge pulse, with pulse energy equivalent to the energy released from the surface discharge, is injected into the circuit model. The circuit model can then be simulated on a transient response circuit analysis program to determine the magnitude of electrical current coupled into the spacecraft equipment.

Analytical Modelling. Research efforts with analytical models are introduced here to conclude this review of charging models. One significant factor involved with modelling is the cost to set up and operate a large

simulation program like NASCAP. This modelling technique can be used to simplify the evaluation of spacecraft surface charging processes and potentials. Order-of-magnitude calculations are possible using analytical techniques. Spacecraft surface material insulation breakdown is one main concern and these breakdown potentials are on the order of hundreds of volts at least. Therefore, order-of-magnitude potential calculations should be adequate for first order breakdown potential analysis.

The spacecraft design guidelines issued by NASA to minimize spacecraft charging indicate that analytical techniques can be used to determine worst case charging for spacecraft (Purvis and others, 1984:3-4). For potentials of greater than 500 volts the NASCAP program should be used to further analyze the charging. Prevention methods may be needed to eliminate the build up of charge in particular areas of a spacecraft. Purvis presents a set of equations to model charging on a spherical spacecraft structure at geosynchronous altitude, and also discusses the use of these equations with a worst case plasma environment.

Higgins presents an analytical approach to evaluating spacecraft charging by using basic two- and three-dimensional geometric models and electrical field theory

(Higgins, 1979:5162-5163). The two dimensional geometry is modelled by a parallel plate capacitor with either a grounded or isolated substrate. An electric dipole field model is used in the grounded substrate case and a monopole term is added for the isolated substrate case. Both models are evaluated to determine the energy required by an electron to reach the charged surface. The surface charge density and electric field strength is approximated for each case, and this shows that the isolated substrate has an electric field intensity which is about three orders of magnitude less than the grounded substrate case. A spherical geometry is also examined and is found to give similar results.

Higgins concludes that the assumption of surface grounding by photoelectron emission is significant and needs to be carefully examined. These charging computations show a reasonable correspondence with NASCAP's three dimensional computer simulation, and perhaps give a better insight into the nature of the surface charging phenomenon.

Garrett reviews the development of spacecraft charging research up to 1981, and summarizes the main factors involved in charging analysis (Garrett, 1981:577-604). This includes charging current mechanisms, probe theory analysis,

and numerical analysis. The analytical probe theory separates the analysis into either thin or thick potential sheath situations depending on the relative size of the spacecraft structure compared to the Debye length. Numerical analysis is considered for complex spacecraft structures where more detailed potential and charge distributions are required.

The charging theory presented by Garrett determines spacecraft surface equilibrium potential from an analysis of the charged particle flux balance at each spacecraft surface. Eq (2.14) represents the total current flux to a surface and is simply the sum of all charged particle currents.

$$I_e - I_i - I_{se} - I_{si} - I_{bs} - I_{ph} = I_t \quad (2.14)$$

where

$I_e$  = electron current (amps)

$I_i$  = ion current

$I_{se}$  = secondary electron emission due to electrons

$I_{si}$  = secondary electron emission due to ions

$I_{bs}$  = backscattered electrons

$I_{ph}$  = photoelectron current

$I_t$  = total current to spacecraft

( $I_t = 0$  at equilibrium)

The surface potential can be computed from Eq (2.12) (Poisson's equation), given the charge density around a spacecraft. However, the surface potential changes as the spacecraft charges to achieve current balance. The electric field due to the surface potential will affect the charge density around the spacecraft in accordance with Eq (2.13) (Vlasov's equation) which will in turn affect the surface potential. Therefore, the surface equilibrium potential is dependent on a self consistent solution of Eq (2.14) subject to the Poisson and Vlasov equations.

Analytic assumptions based on plasma probe theory have been used to simplify the solution of this current balance equation. When the Debye length is short compared to a spacecraft size the potential sheath is close to the spacecraft, and the sheath is assumed to dominate the current flow at the spacecraft surface. Therefore, Poisson's equation is significant because it relates the surface potential to the space charge in the sheath region. In the thick sheath case, however, the Debye length is large compared to the spacecraft dimensions. In this case the space charge can be neglected, and this assumption simplifies Poisson's equation (Garrett, 1981:593-596). At geosynchronous altitude, for a worst case plasma environment, the Debye length is large (about 0.7Km);

therefore, the thick sheath assumption is valid for this charging case.

The current balance equations presented in NASA's charging guidelines are an analytical derivation for the thick sheath case (Purvis and others, 1984:4; Garrett, 1981:594-597). Eq (2.14) and Eqs (2.15) to (2.20) form a first order current density model for charging on one surface of a three-dimensional spacecraft in a single Maxwellian plasma environment. The current density terms are functions of surface potential and plasma particle characteristics. Garrett cites this charging model and also presents another more general, but equivalent, set of equations for the three-, two-, and one-dimensional surface charging cases.

Garrett also reviews charging current mechanisms, including photoelectron emission, backscattering, and secondary electron emission (Garrett, 1981:585-589). The characteristic response of aluminium, to these charging processes, is specified from experimental research. The review also indicates that the actual response of materials in space is not well known. This lack of knowledge of spacecraft materials contamination is identified as a major shortfall in charging analysis.

For electrons:

$$J_e = J_{eo} \exp(qV/KT_e) \quad V < 0 \text{ repelled} \quad (2.15)$$

$$J_e = J_{eo}(1 + (qV/KT_e)) \quad V > 0 \text{ attracted} \quad (2.16)$$

For ions:

$$J_i = J_{io} \exp(-qV/KT_i) \quad V > 0 \text{ repelled} \quad (2.17)$$

$$J_i = J_{io}[1 - (qV/KT_i)] \quad V < 0 \text{ attracted} \quad (2.18)$$

$$J_{eo} = (qN_e/2)(2KT_e/\pi m_e)^{0.5} \quad (2.19)$$

$$J_{io} = (qN_i/2)(2KT_i/\pi m_i)^{0.5} \quad (2.20)$$

where

$J_e$  = electron current density (amp/m<sup>2</sup>)

$J_i$  = ion current density

Analytic probe theory has applications in some practical problems and simple spacecraft geometries; however, the quantitative accuracy is limited when complex structures are examined. Accurate calculations have been obtained by using numerical methods to solve more complex forms of the self consistent charging problem. One example of a more rigorous numerical solution is the three dimensional NASA charging analyzer program (NASCAP) that has been discussed here.

### III. METHODOLOGY

This chapter gives the methodology used to evaluate spacecraft charging as a source of electrical energy for spacecraft. Research is done to specify the geosynchronous plasma environment and a suitable spacecraft surface charging model. Surface potentials on isolated sections of the spacecraft structure are then computed and examined. The differential potentials, produced by surface charging, are identified as possible sources of energy. An electrical current path between differentially charged surfaces is included in the charging model to determine the discharge current that will flow between charged spacecraft surfaces. The power available through this discharge current path is examined as a possible supplement to other spacecraft power sources.

#### Geosynchronous Plasma Environment

Environmental conditions for spacecraft charging at geosynchronous orbit are obtained from satellite experiments and data analysis. The worst case environment generally occurs during geomagnetic substorm conditions between local midnight and dawn in the spacecraft orbit. Plasma conditions are specified here for both worst case substorm and average plasma conditions.

### Charging Model

The spacecraft charging model selected is based on plasma probe theory, and uses a charged particle flux balance equation to represent the flux of plasma particles at each surface of the spacecraft. Fig 3.1 illustrates the physical and electrical form of the spacecraft charging model.

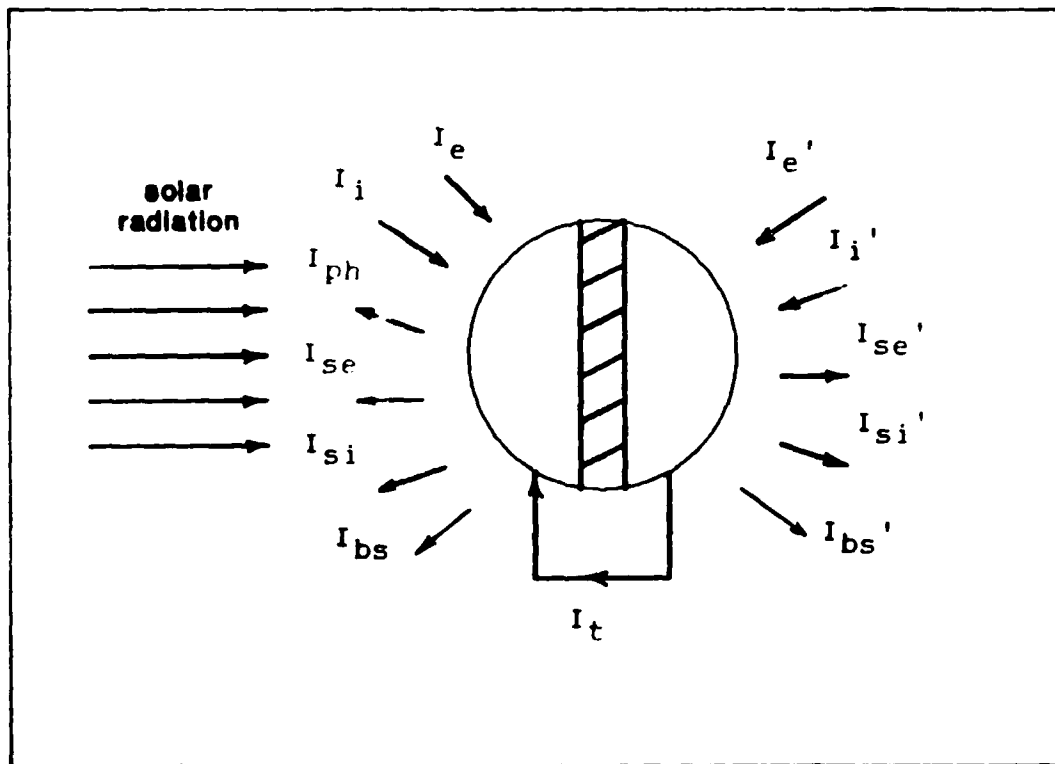


Fig 3.1 Spacecraft Charging Model

A simplified spherical spacecraft structure is used: consisting of two electrically isolated hemispheres of conductive material. This surface structure allows an

analytical solution to be implemented, giving first order estimates of equilibrium surface potentials. A simple plasma current density equation is also used to compare the maximum current flow available from the plasma environment to the current available from the spacecraft charging model.

The charging model includes terms for plasma electron and ion current, photoelectron emission, secondary electron emission, and backscattered electrons. Variations in photoelectron emission occur during eclipse of the spacecraft by the earth and spacecraft spin. These variations are included by modifying terms in the charging equations. Attenuation of solar radiation by the earth's atmosphere will be neglected here. Plasma conditions are varied by substituting either the worst case or average plasma characteristics into the charging equations.

A surface discharge current  $I_t$  is modelled by introducing a current flow term in the charging equations for each surface. This current is effectively drawn from one surface and added to the other. The discharge current electrically couples the two surfaces; therefore, any increase in the discharge current reduces the potential difference between the surfaces. The maximum current occurs when the potential difference is reduced to zero. This

maximum discharge current represents the approximate current sourcing ability of the spacecraft charging process in a given plasma environment.

Application of the Charging Model

In this section the charging model is used to determine surface potentials that occur for each discharge current, plasma environment, and spacecraft orientation. The resultant surface potentials are evaluated and discussed in relation to the discharge current capacity of the spacecraft charge, and the use of charge as a source of electrical power.

#### IV. GEOSYNCHRONOUS PLASMA ENVIRONMENT

The plasma environment is defined here for spacecraft charging calculations under worst case and average plasma conditions. Plasma can be specified by a particle distribution function which depends on particle density and energy. At geosynchronous altitude this plasma distribution is complicated by the effects of solar wind on the earth's magnetic field.

NASA spacecraft charging guidelines (Purvis and others, 1984:1-42) use a worst case geosynchronous plasma environment in calculations to determine if a particular spacecraft surface potential exceeds about 500 Volts. This potential is estimated as the minimum potential for arc discharge hazard. The worst case plasma environment results from solar wind disruption of the magnetosphere which causes geomagnetic substorm activity. These substorms can inject high energy, low density plasma into the path of geosynchronous spacecraft.

Table 4.1 gives the worst case plasma environment used by the NASA spacecraft charging guidelines. This environment is also used here to specify maximum charging conditions (90% single Maxwellian distribution).

Table 4.1 Worst Case Geosynchronous Plasma Environment

|                         |       |   |                     |                 |
|-------------------------|-------|---|---------------------|-----------------|
| Electron Number Density | $N_e$ | = | $1.12 \times 10^6$  | $\text{m}^{-3}$ |
| Electron Temperature    | $T_e$ | = | $1.2 \times 10^4$   | eV              |
| Ion Number Density      | $N_i$ | = | $0.236 \times 10^6$ | $\text{m}^{-3}$ |
| Ion Temperature         | $T_i$ | = | $2.95 \times 10^4$  | eV              |

(Purvis and others, 1984:3)

The single Maxwellian plasma may not be accurate under all plasma extremes, or under the shielding effects of a charged spacecraft surface. But, the representation is considered adequate for first order analytical charging computations (Purvis and others, 1984:3; Garrett, 1981:586).

The worst case charging environment gives the best conditions for surface charge collecting. However, these conditions are not present during the entire orbit of a geosynchronous satellite. Average plasma conditions have been determined by averaging the measurements from spacecraft experiments. Table 4.2 specifies an average plasma environment from ATS-5 satellite measurements. Purvis shows that average plasma values are known to vary greatly with the standard deviation often exceeding the average value. Average plasma values also vary yearly with solar cycles. The average environment given in Table 4.2 is

used here to represent pre-substorm conditions and hence the initial plasma environment.

Table 4.2 Average Plasma Environment: ATS-5 (1969-1970)

|                         |       |   |                   |                 |
|-------------------------|-------|---|-------------------|-----------------|
| Electron Number Density | $N_e$ | = | $0.8 \times 10^6$ | $\text{m}^{-3}$ |
| Electron Temperature    | $T_e$ | = | 1.85              | eV              |
| Ion Number Density      | $N_i$ | = | $1.3 \times 10^6$ | $\text{m}^{-3}$ |
| Ion Temperature         | $T_i$ | = | 6.8               | eV              |

(Purvis and others, 1984:3)

Plasma conditions can change significantly over a 24 hour orbit period due to substorm activity. Spacecraft in the local midnight to dawn time period are known to be most susceptible (McPherson, 1976:16-21). The plasma conditions used here are assumed to be average from 0600 to midnight local time, and worst case plasma for the remaining six hours.

## V. CHARGING MODEL

This chapter presents the development of a charged particle current balance model to examine the effects of charging on the surfaces of a geosynchronous spacecraft. A simple plasma flux density equation is also given to determine approximate maximum current densities from a plasma environment. This probe equation is used for comparison with surface charging model results. Surface potentials are computed with the charging model for a spherical spacecraft structure with both environmental plasma and solar irradiation variations. A surface discharge current is also included in the model to examine the magnitude of current that can flow between differentially charged surfaces, and the effect this current has on spacecraft surface potentials. The suitability of this discharge current as a source of energy is of interest here.

The current balance model has been developed from plasma probe theory by considering the spacecraft as a probe in plasma. This modelling technique forms the basis of the three dimensional spacecraft charging analyzer program (NASCAP) developed for NASA. A thick potential sheath assumption is valid for geosynchronous altitude which can

simplify the solution of the charging problem to an analytical form when a simple spacecraft structure is used. The analytical model is considered to be a reasonable first order approximation to determine worst case charging potentials under the NASA charging guidelines (Purvis and others, 1981:3-4).

One equation is used to represent charging at each spacecraft surface. The external spacecraft structure is modelled by a one metre radius sphere with two electrically isolated hemispheres constructed of aluminium. A conductive sphere charges in about  $10^{-3}$  seconds in the magnetospheric plasma. Therefore, surface potential fluctuations can be considered static compared to plasma changes, which generally occur over minutes or longer (Garrett, 1981:584-585). This implies that the surface potential variations on a conductor surface will effectively occur in time with plasma changes.

#### Plasma Flux Density

Charged particle current density to an isolated surface in plasma can be estimated by Eq (5.1) (one dimensional case) (Chapman, 1980:51-53). This equation gives the maximum current density from plasma with a given particle energy and density.

$$J = qNv_{av} \quad (\text{amp/m}^2) \quad (5.1)$$

The number of charged particles that can be drawn from a plasma is limited to the density of particles in the region of the surface. Therefore, a spacecraft's surface current sourcing ability can be approximated from Eq (5.1). If only ions collect on the surface material, then the surface potential will be positive; electron collection will cause a negative surface potential. For a given plasma particle density the electrons have higher velocities. This implies that the current density due to electrons will be higher. Therefore, an isolated surface in plasma charges to some negative potential. Charge balance on a surface is achieved when the negative surface potential and the ion flux balances the higher flux of electrons.

Eq (5.1) does not account for the repulsion of particles from a charged surface, the secondary electron emission, or the backscattered electrons. But, estimates of the maximum current densities due to electrons and ions can be determined from this one equation. Therefore, Eq (5.1) is used here as a guide to current collection calculations. Table 5.1 gives approximate maximum current densities for the geosynchronous plasma environment specified in Chapter IV.

Table 5.1 Plasma Current Density at Geosynchronous Altitude

| Worst Case Plasma |   |  |
|-------------------|---|--|
| $J_e$             | = | $13.1 \times 10^{-6}$ amp/m <sup>2</sup> |
| $J_i$             | = | $0.1 \times 10^{-6}$ amp/m <sup>2</sup>  |
| Average Plasma    |   |  |
| $J_e$             | = | $0.11 \times 10^{-6}$ amp/m <sup>2</sup> |
| $J_i$             | = | $8.3 \times 10^{-9}$ amp/m <sup>2</sup>  |

Charging Model Current Terms

The charged particle currents to each isolated spacecraft surface can be represented by Eq (5.2) (Garrett, 1981:592-600; Purvis and others, 1984:4).

$$I_e - I_i - I_{se} - I_{si} - I_{bs} - I_{ph} = I_t \quad (5.2)$$

This equation models the total flux to a surface from plasma electrons and ions, photoelectron emission, secondary electron emission, and backscattered electrons. When the spacecraft surface is charged to an equilibrium potential the total current to the surface  $I_t$  is zero. The solution of Eq (5.2) for an equilibrium surface potential and charge density is subject to the constraints of Poisson's equation (Eq (2.12)) and the Vlasov equation (Eq (2.13)) in a self-consistent way. Solving this problem normally requires an

iterative numerical process using a grid pattern of the spacecraft surface structure and the surrounding space. However, the problem can be simplified at geosynchronous altitude because, at this altitude, the Debye length (Eq (5.3)) is large compared to the spacecraft dimensions used here (the thick sheath case).

$$\lambda_d = (\epsilon_0 kT/q^2 N_0)^{0.5} \quad (\text{metres}) \quad (5.3)$$

The thick sheath case neglects the space charge term in Eq (2.12), and this assumption allows an analytic solution to Eq (5.2) to be obtained. Table 5.2 gives Debye lengths for the plasma specified in Chapter IV.

Table 5.2 Debye Lengths for Geosynchronous Environment

| <u>Plasma</u> | <u>Particle Density <math>N_0</math></u> | <u>Debye Length (metres)</u> |             |
|---------------|--|------------------------------|-------------|
|               |  | <u>Electrons</u>             | <u>Ions</u> |
| Worst Case    | $1.34 \times 10^6 \text{ m}^{-3}$        | 1100                         | 700         |
| Average       | $2.1 \times 10^6 \text{ m}^{-3}$         | 13.4                         | 7           |

The analytic approach gives surface current densities in the form of Eqs (5.4) to (5.9). These densities are dependent on the spacecraft equilibrium surface potential. The equations are valid for the thick sheath case with a

spherical spacecraft geometry and an isotropic Maxwellian plasma distribution. Eqs (5.4) to (5.7) show the variation of surface current density to a charged surface as a function of surface potential. Eqs (5.8) and (5.9) are equivalent to Eq (5.1) for electrons and ions when using an isotropic Maxwellian particle distribution.

For electrons:

$$J_e = J_{eo} \exp(qV/KT_e) \quad V < 0 \text{ repelled} \quad (5.4)$$

$$J_e = J_{eo} [1 + (qV/KT_e)] \quad V > 0 \text{ attracted} \quad (5.5)$$

For ions:

$$J_i = J_{io} \exp(-qV/KT_i) \quad V > 0 \text{ repelled} \quad (5.6)$$

$$J_i = J_{io} [1 - (qV/KT_i)] \quad V < 0 \text{ attracted} \quad (5.7)$$

$$J_{eo} = (qN_e/2)(2KT_e/\pi m_e)^{0.5} \quad (5.8)$$

$$J_{io} = (qN_i/2)(2KT_i/\pi m_i)^{0.5} \quad (5.9)$$

Photoelectron Emission. Solar radiation incident on the exposed spacecraft surfaces causes photoelectron emission. This emission is dependent on the flux of solar radiation, surface material, and spacecraft surface potential. Eqs (5.10) and (5.11) give the current density of photoelectrons leaving a charged surface (Massaro and others, 1977:244-245).

$$J_{ph} = J_{pho} \exp(-qV/KT_{ph}) \cos(x) \quad V > 0 \quad (5.10)$$

$$J_{ph} = J_{pho} \cos(x) \quad V < 0 \quad (5.11)$$

where

$J_{ph}$  = photoelectron current density (amps/m<sup>2</sup>)

$J_{pho}$  = total photoelectron current density (amps/m<sup>2</sup>)  
(normal incidence)

$T_{ph}$  = photoelectron temperature (°K)

$x$  = angle of incidence of solar radiation (degrees)

Values of  $J_{pho} = 2nA/cm^2$ , and  $q/KT_{ph} = 1/3$  are used here for an aluminium surface material (Garrett, 1981:586-587, 611).

Secondary Electron Emission and Backscatter. Electrons and ions incident on a spacecraft surface cause electrons to leave the surface (secondary electron emission). Incident electrons are also backscattered (reflected) from the surface material. The secondary emission and backscatter parameters given in Table 5.3 have been determined from experiments with aluminium. These values represent the number of electrons leaving a surface per incident particle. The parameters in Table 5.3 are valid for a zero or negative surface potential, but they can be neglected when the surface potential is positive (Garrett, 1981:589). A positive potential tends to re-attract the electrons to the surface.

Table 5.3 Secondary Emission and Backscattered Electron  
Parameters for Aluminium

|                                     |        |   |     |
|-------------------------------------|--------|---|-----|
| Secondary due to incident electrons | $s_i$  | = | 3   |
| Secondary due to incident ions      | $s_e$  | = | 0.4 |
| Backscattered electrons             | $BS_e$ | = | 0.2 |

(Purvis and others, 1984:4)

Surface Charging Model Development

The model developed for this charging application uses Eq (5.2) and Eqs (5.4) to (5.11), and the parameters introduced above to construct a surface charging model. This model is formed by collecting the appropriate potential current density terms, depending on the surface potential, for substitution into Eq (5.2). The spacecraft is considered to be spin-stabilized in geosynchronous orbit. However, a body-stabilized condition is simulated by zero rotation in this model. The model is used to solve for surface potentials while simulating discharge currents between spacecraft surfaces in sunlit and eclipsed locations in orbit. Plasma conditions are changed for each orbit location. Sunlit and eclipse are considered as distinct applications of the model because the charging equations involve photoelectron emission in the sunlit case but not in the eclipse case.

The surface potential polarity determines the current density terms selected to model the charging of each surface, and the balance of particle currents gives the surface potential. Plasma particles are exposed to all surfaces of the spacecraft, but photoelectron emission only occurs on surfaces exposed to solar radiation.

Photoelectron current can dominate plasma current at geosynchronous altitudes which is likely to give positive potentials on the exposed surfaces (McPherson and Schrober, 1976:19). For shaded surfaces, however, plasma charging is dominated by the electrons. Therefore, negative potentials are expected on an isolated surface in plasma (Chapman, 1980:51-52).

The surface area of a spinning spacecraft exposed to solar radiation changes during rotation. The product of the current density terms and the exposed surface area gives the particular charging current. Therefore, surface potential polarities are likely to change with spacecraft rotation. Eq (5.13) represents the fraction of the effective surface area, of one hemisphere of the spacecraft, exposed to the sun as it rotates. This equation is obtained by integrating and normalizing the surface area of the shaded hemisphere, irradiated by the sun, as a function of the rotation angle  $\theta$ . Eq (5.13) is only valid for  $\theta$  in the range of  $-\pi/2$  to

$\pi/2$ . The maximum effective surface area of a hemisphere illuminated by the sun is the area of a circle with the same radius as the sphere. Zero degrees rotation has one surface completely exposed and the other shaded. Any rotation will decrease the area exposed on one side and increase it on the other side.

$$F = 1/2 + (\sin^2(\pi/2 - \theta))/2 \quad (5.13)$$

where

$F$  = fraction of area exposed ( $F = 1$ , for  $\theta = 0$ )

$\theta$  = angle of rotation from totally exposed

One current balance equation is used to model charging on each hemisphere of the spacecraft. A current discharge path between the two charging surfaces is modelled by the electron current  $I_t$  in Eq (5.2).  $I_t$  is added to the balance equation that results in the higher positive potential, and is subtracted from the other equation to simulate a discharge current between the surfaces. When the potential difference between the surfaces is reduced to zero the discharge current is at a maximum. Therefore,  $I_t$  approximates the current that may be sourced by a spacecraft at geosynchronous altitude.  $I_t$  also represents the current flow needed between the two surfaces to eliminate a charge buildup.

Eq (5.14), (5.15), and (5.16) are used here to model the current flow to a rotating spacecraft exposed to solar radiation.

V Positive

$$AJ_{eo}[1 + (qV/KT_e)] - AJ_{io}\exp(-qV/KT_i) - FA_{ph}J_{ph}\exp(-qV/KT_{ph}) + I_t = 0 \quad (5.14)$$

V Negative

$$AJ_{eo}(1 - S_e - BS_e)\exp(qV/KT_e) - AJ_{io}(1 + S_i)[1 - (qV/KT_i)] - (1 - F)A_{ph}J_{ph} - I_t = 0 \quad (5.15)$$

V Positive

$$AJ_{eo}[1 + (qV/KT_e)] - AJ_{io}\exp(-qV/KT_i) - (1 - F)A_{ph}J_{ph}\exp(-qV/KT_{ph}) - I_t = 0 \quad (5.16)$$

where

$A$  = surface area exposed to incident particles

$A_{ph}$  = effective surface area irradiated by sunlight

Eq (5.14) models the current balance on the hemisphere initially exposed to the sun, and Eq (5.15) models the side that is shadowed. As the spacecraft rotates the shaded side has more surface area exposed to the sun and will change from a negative to positive potential. Eq (5.15) is only defined for a negative surface potential and is replaced by Eq (5.16) when the surface potential changes to a positive

value. As the rotation reaches 90 degrees the potential on the initially shaded side will equal the exposed side because equal areas are exposed to the sun. For a spherical spacecraft the surface charging is symmetrical; therefore, 90 degrees of rotation is sufficient to compute all surface potentials required here.

Only plasma currents occur in eclipse conditions which means that an absolute (overall) negative surface potential will result. Therefore, Eq (5.15) can be used to represent charging on both hemispheres in eclipse conditions.

## VI. APPLICATION OF THE CHARGING MODEL

Charging simulation results are presented and discussed in this section. Analysis includes charging on a surface stabilized spacecraft and also a rotating spacecraft. Both spacecraft models are exposed to sunlight and eclipse conditions, and also the effects of worst case and average plasma environments. The charging model is solved using the equation solver routines in MATHCAD 2.0: an engineering computer software package by MathSoft Inc. The Appendix lists the problem formulated as a MATHCAD document. The output data from MATHCAD 2.0 has been graphed using the spreadsheet QUATTRO by Borland.

### Plasma Current Density

Table 5.1 specifies the approximate maximum current densities expected from the plasma environment. The maximum plasma current to a surface, given by Eq (6.1), is the product of the plasma current density (Eq (5.1)) and the surface area exposed to plasma.

$$I = AqNV_{av} \quad (6.1)$$

where

$$I = \text{current to surface (amps)}$$

Table 6.1 gives the plasma current to one hemisphere of the spacecraft. These maximum expected currents are small and would have limited use as a power source. The values indicate that large surface areas would be required to produce significant plasma currents.

Table 6.1 Maximum Plasma Current to One Surface of the Spacecraft

**Worst Case Plasma**

$$I_e = 82.3 \times 10^{-6} \text{ amps}$$

$$I_i = 0.63 \times 10^{-6} \text{ amps}$$

**Average Plasma**

$$I_e = 0.69 \times 10^{-6} \text{ amps}$$

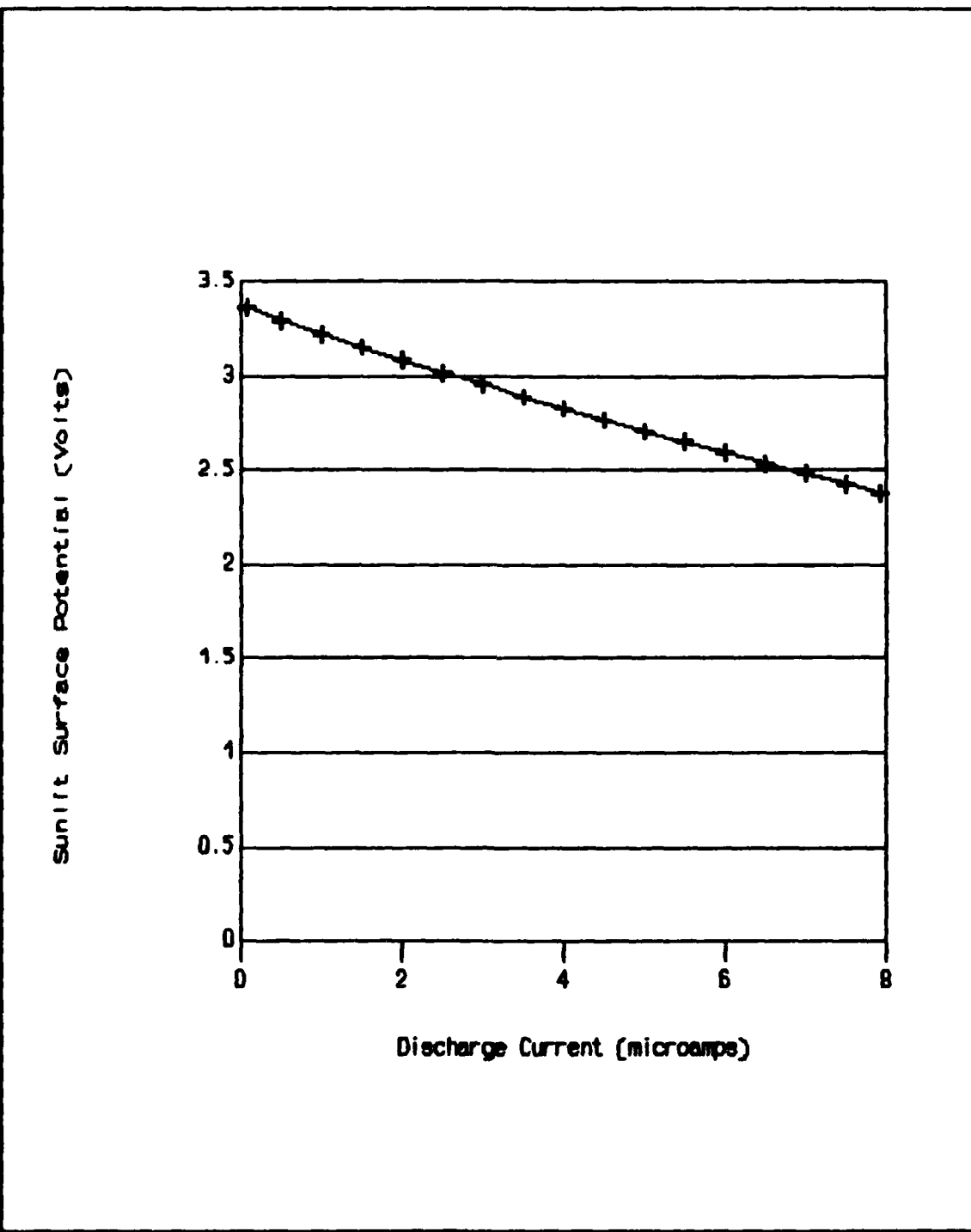
$$I_i = 52.1 \times 10^{-9} \text{ amps}$$

**Charging in Sunlit Conditions - Worst Case Plasma**

In this section surface potential plots are presented and discussed for a range of spacecraft orientations and simulated discharge currents. Symmetry exists in the spherical model so the plots are valid for rotations beyond the 90 degrees displayed. For further rotation the equations can be exchanged to represent charging on the opposite surface.

Figs 6.1 and 6.2 display surface potentials as a function of discharge current for the spacecraft at zero degrees of rotation. In this orientation one side is fully exposed to the sun and the other is shaded; therefore, maximum surface potentials occur on each surface. Fig 6.2 shows the large negative potential that develops on the shaded surface. However, changes in discharge current as small as only  $10^{-6}$  amps are sufficient to decrease the surface potential by thousands of volts. Fig 6.3 indicates that the maximum current between surfaces occurs when the discharge current  $I_t$  causes the potential difference between the two surfaces to decrease to zero. From Fig 6.3 the maximum discharge current is about  $7.5 \times 10^{-6}$  amps.

One significant factor evident from these graphs is the small positive surface potential on the sunlit surface. This potential varies slightly over the range of discharge currents compared to the shaded side. At maximum  $I_t$  photoelectron current holds the overall surface potential at about +2 Volts. The suppression of surface potential is caused by the dominance of photoelectron emission over plasma currents. Photoelectron emission effects are more completely described in a detailed numerical solution of the charging problem (LaFramboise and others, 1988:711-715).



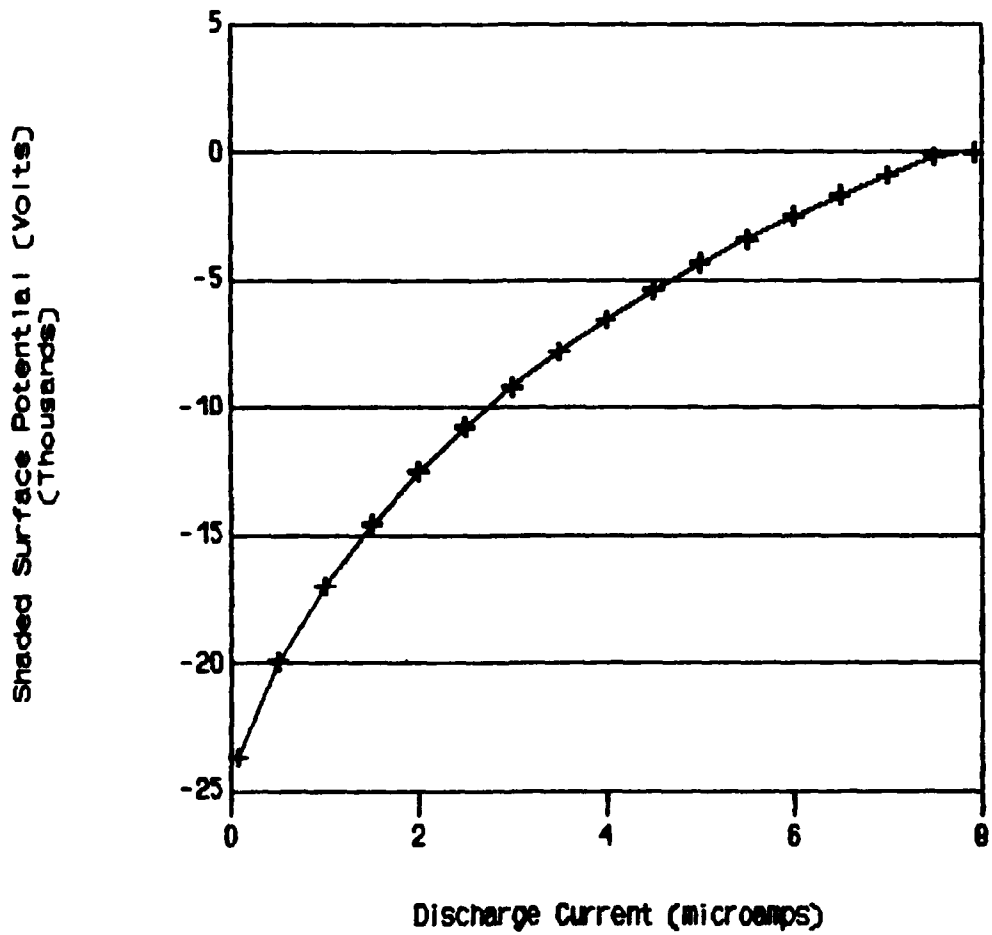


**Fig 6.2 Shaded Surface Potential in Worst Case Plasma - No Rotation**

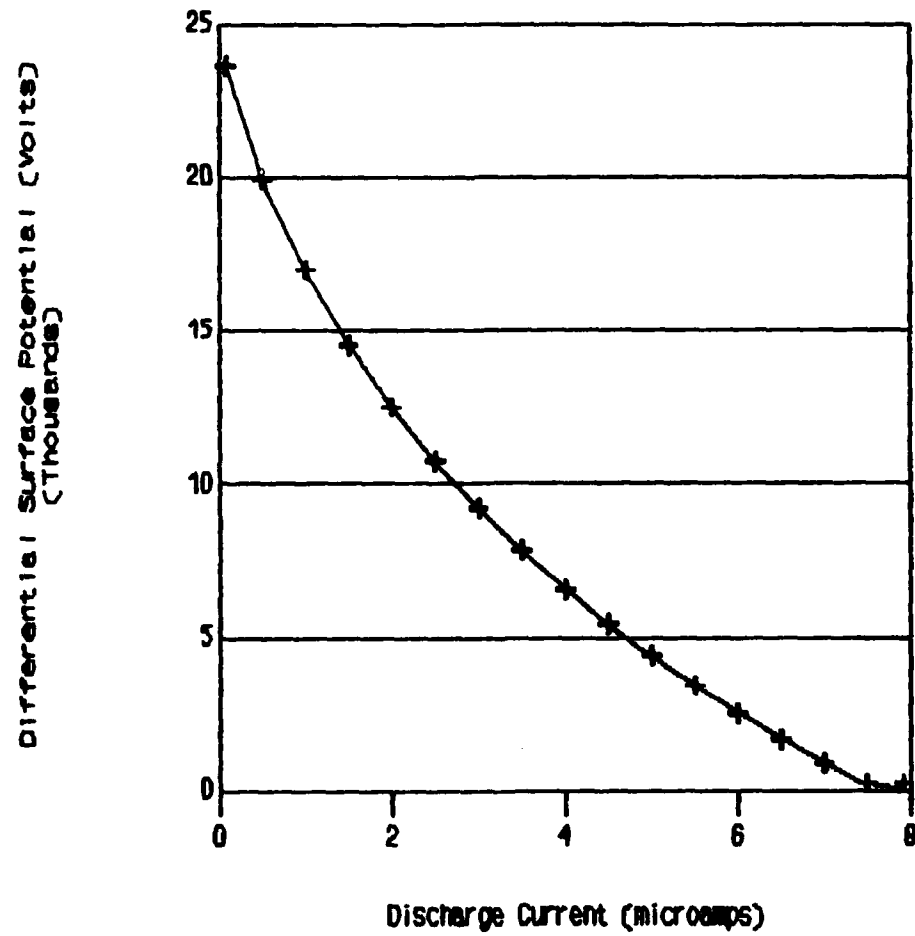


Fig 6.3 Differential Surface Potential in Worst Case Plasma  
-No Rotation

Figs 6.4 to 6.8 describe the change in the sunlit and shaded surface potentials when the spacecraft is rotated so that sunlight illuminates more of the shaded surface. The side with more surface area exposed to the sun has the most positive potential. The limit of discharge current for any orientation occurs when the surface potential difference is zero. This is the reason why the discharge current curves, in Figs 6.4 and 6.6, stop in the middle of the graph.

Fig 6.4 shows the same small potential variation evident in Fig 6.1. However, Fig 6.5 shows that the shaded surface potential changes rapidly up to 30 degrees of rotation where the potential difference across the spacecraft surface is less than 5 volts. At 30 degrees rotation the area of the shaded side that is exposed to sunlight is only 1/7 of the sunlit side. This shows the dominance of photoelectron current over plasma current.

Surface potentials on the shaded side, for 30 to 90 degrees of rotation, are scaled up in Fig 6.6. A plot of the potential difference between surfaces is given in Figs 6.7 and 6.8. This figure shows that for a discharge current of  $7 \times 10^{-6}$  amps the potential difference is small by about 10 degrees of rotation. Fig 6.8 shows that the sunlit and

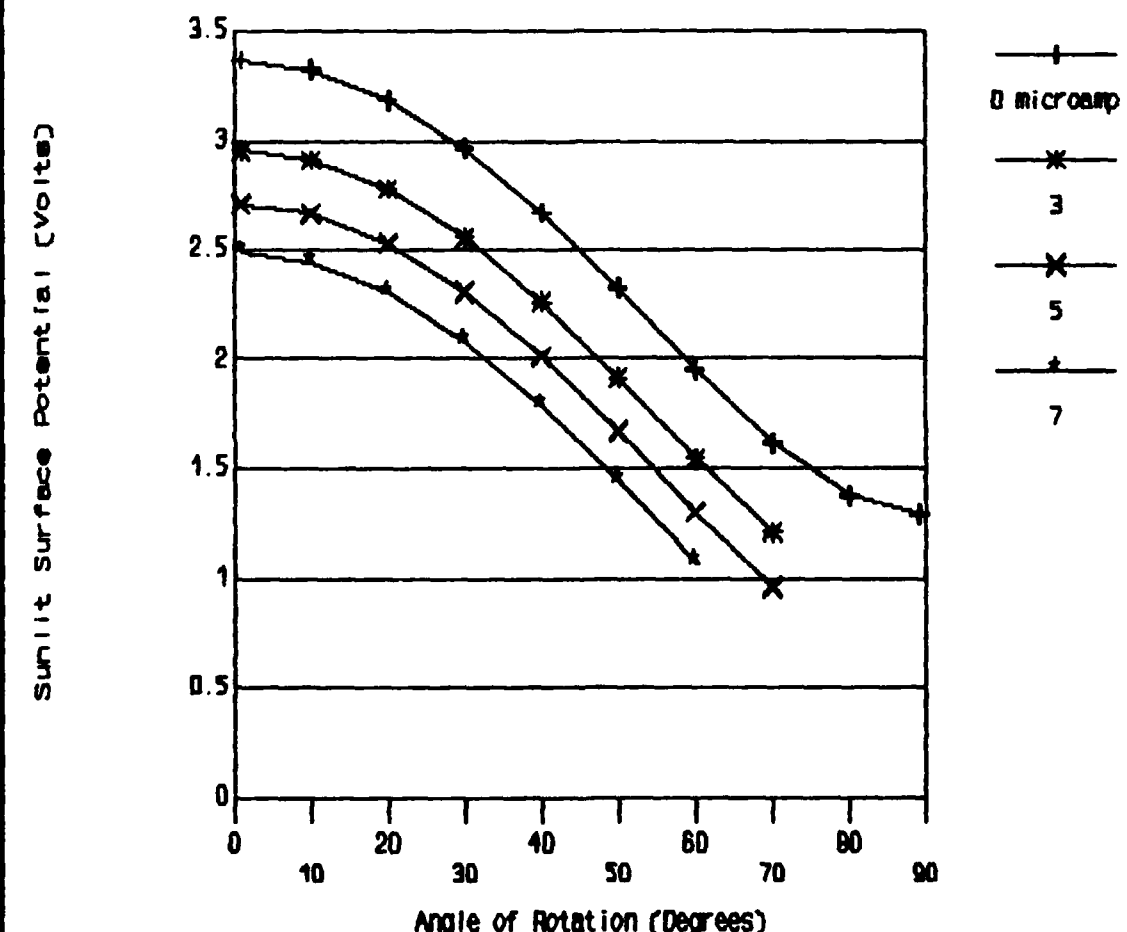


Fig 6.4 Discharge Current Effect on Sunlit Surface Potential in Worst case Plasma for Rotating Spacecraft

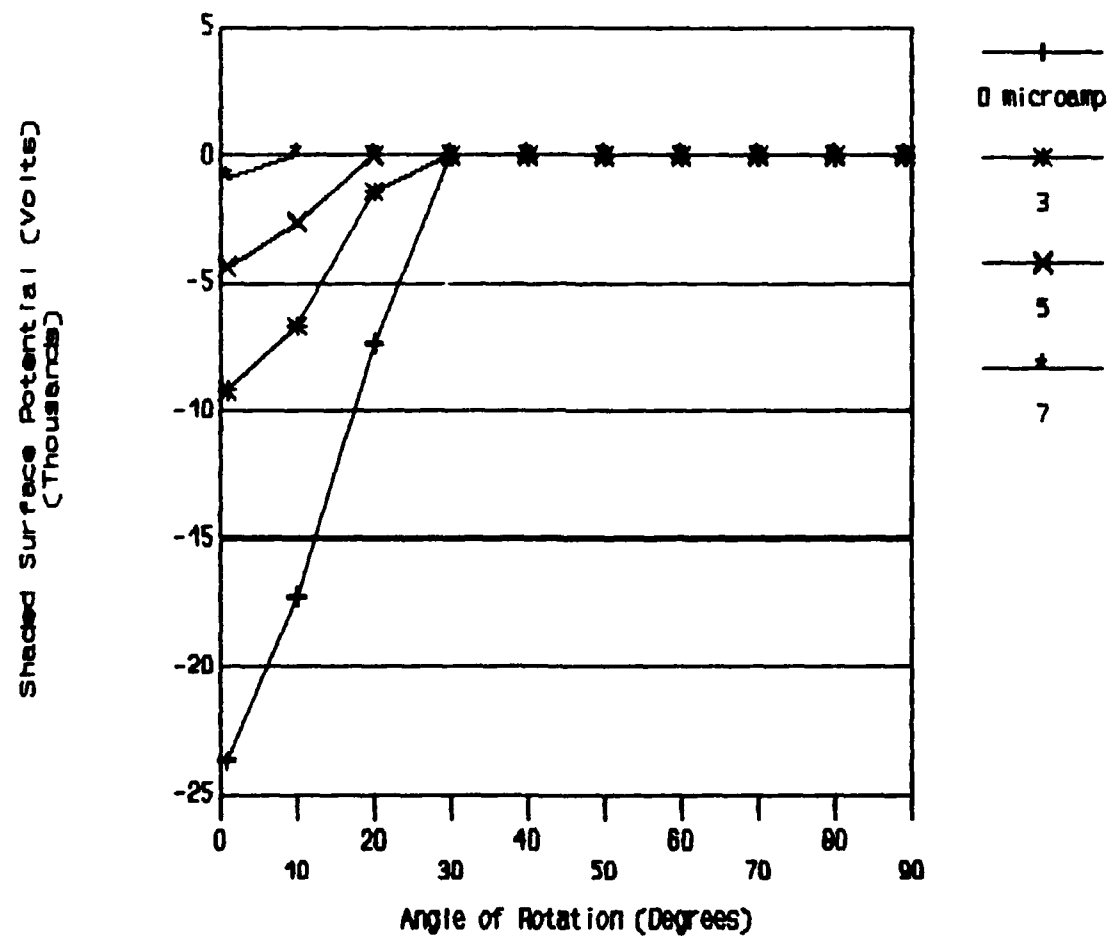


Fig 6.5 Discharge Current Effect on Shaded Surface Potential in Worst Case Plasma for Rotating Spacecraft

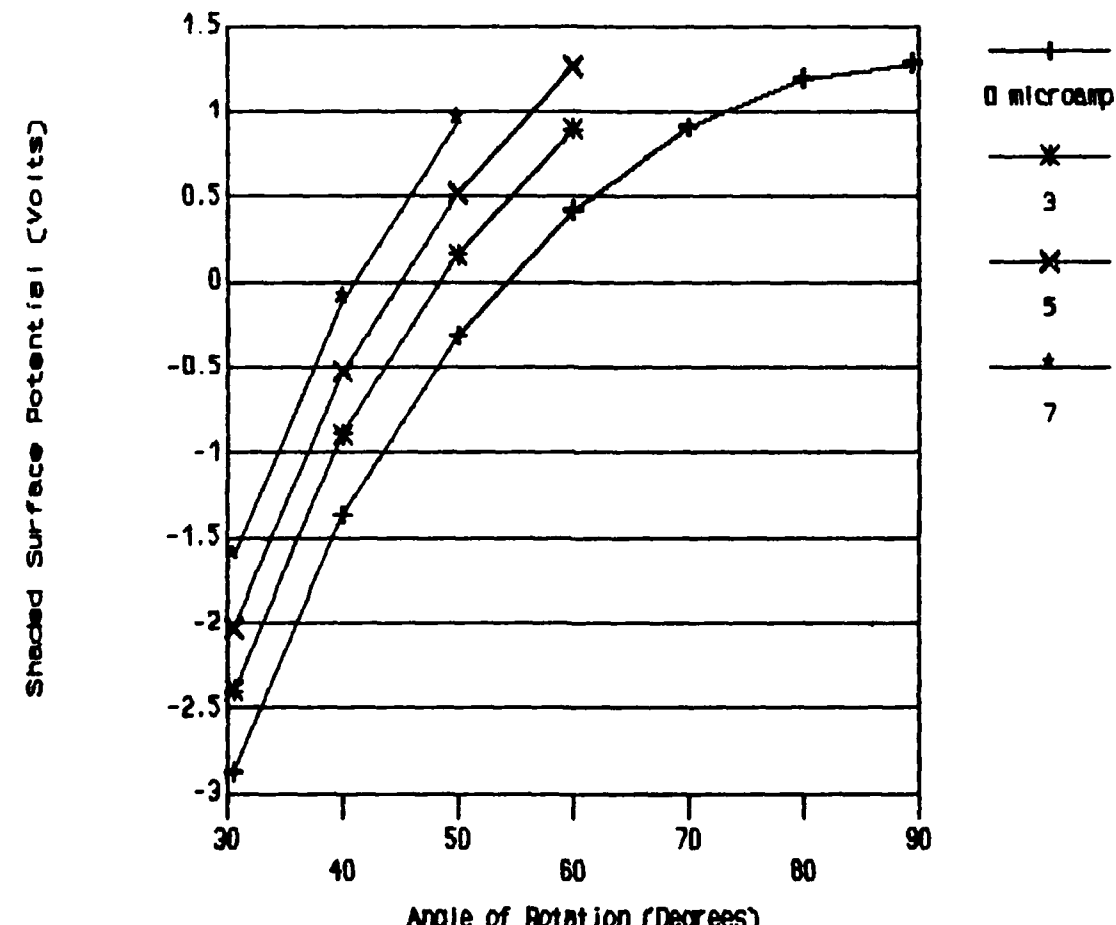


Fig 6.6 Discharge Current Effect on Shaded Surface Potential in Worst Case Plasma for Rotating Spacecraft

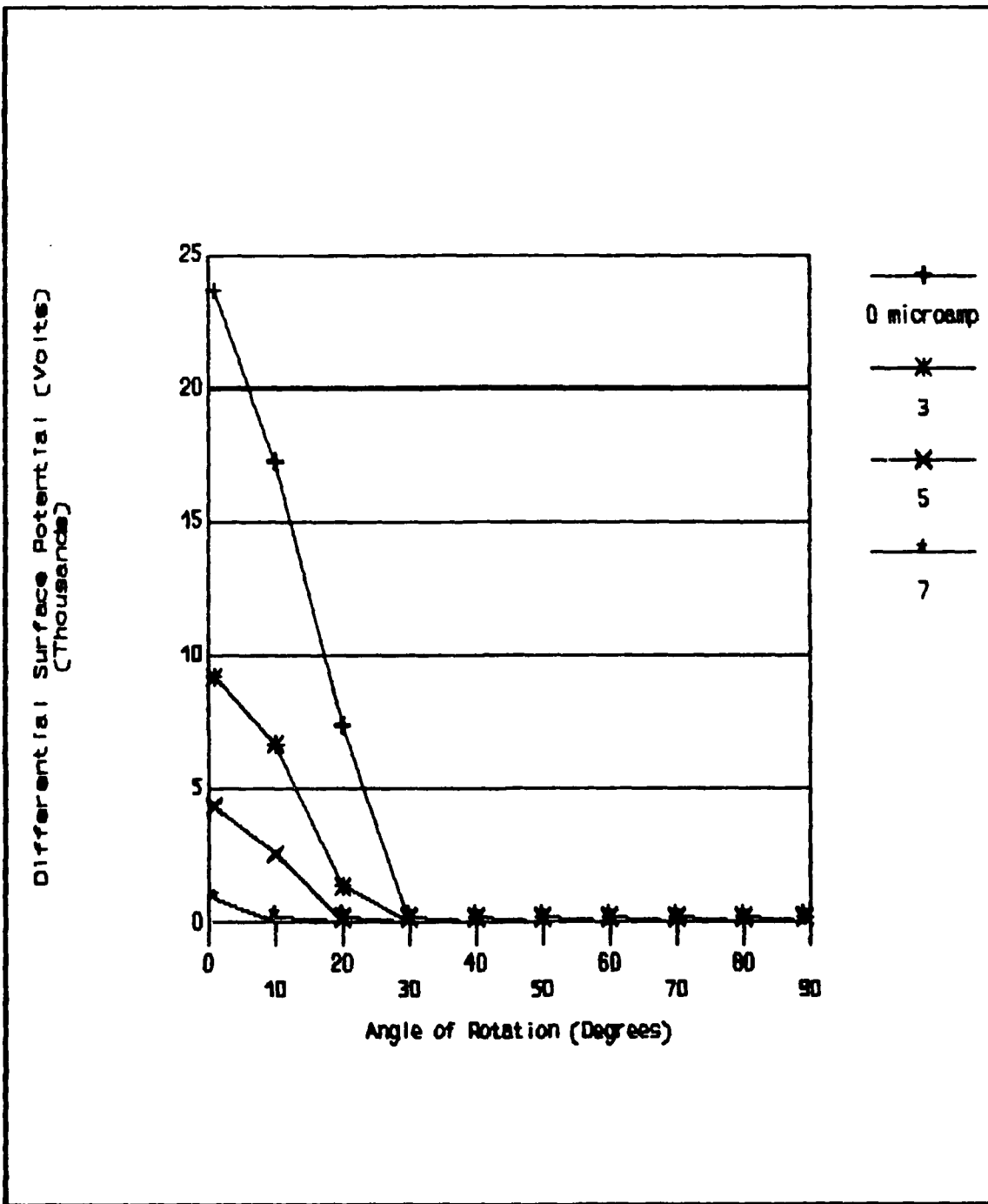


Fig 6.7 Differential Surface Potential in Worst Case Plasma for Rotating Spacecraft

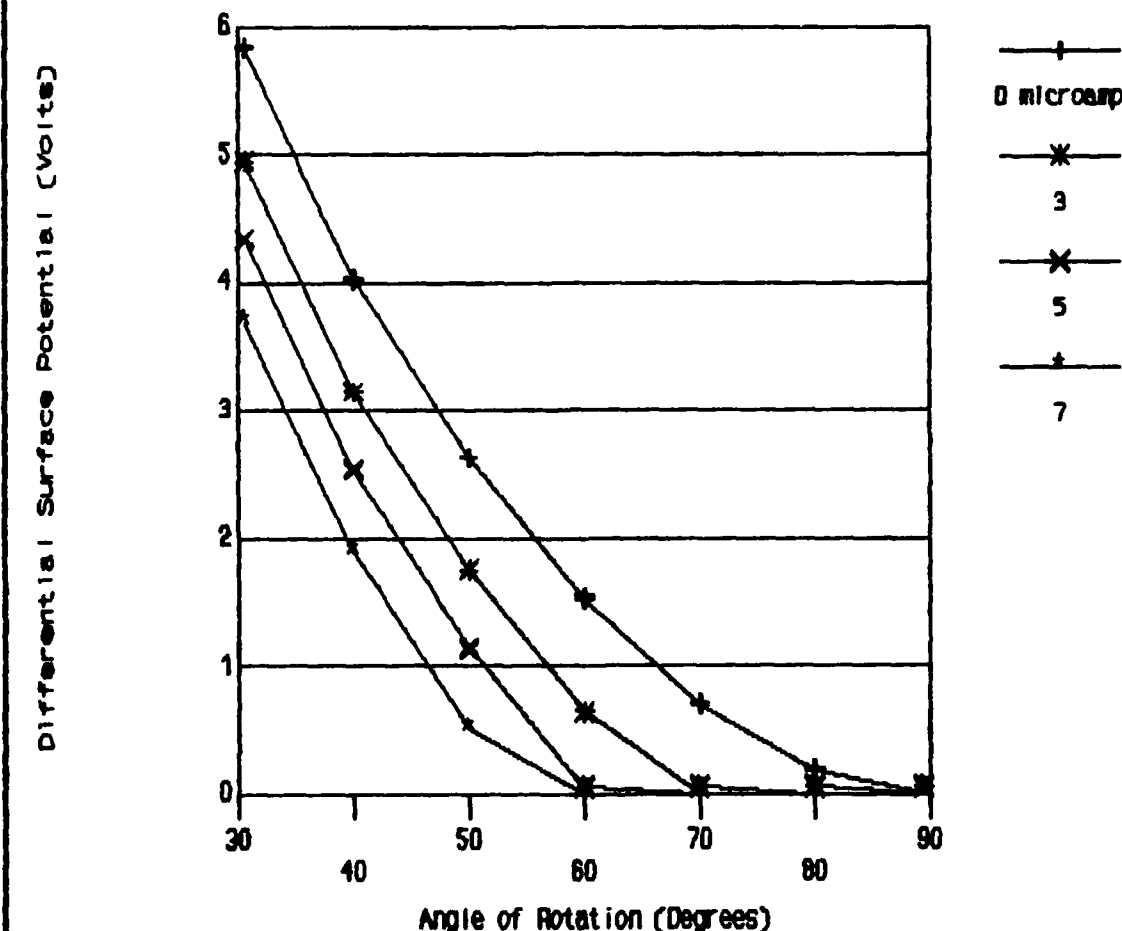


Fig 6.8 Differential Surface Potential In Worst Case Plasma for Rotating Spacecraft

shaded potentials approach the same value at about 60 degrees of rotation.

These results show that the maximum continuous discharge current occurs when one spacecraft surface is sunlit and the other is totally shaded. The maximum current under worst case plasma conditions is likely to be about 7 microamps.

#### Charging in Sunlit Conditions - Average Plasma

This section presents the charging computations using the average plasma environment. Figs 6.9 and 6.10 are for the surface stabilized case, and Figs 6.11 to 6.13 extend the results to the rotating case. Fig 6.9 shows that for the average plasma negative surface charging is negligible, but the sunlit side has about three times the surface potential of the worst case plasma. This implies that photoelectron flux is able to dominate plasma flux even more in the average environment due to the lower plasma particle energies. The differential potential of about 12 volts reduces to zero for a discharge current of about  $10^{-6}$  amps. This current is only about 1/7 of that available for the worst case plasma.

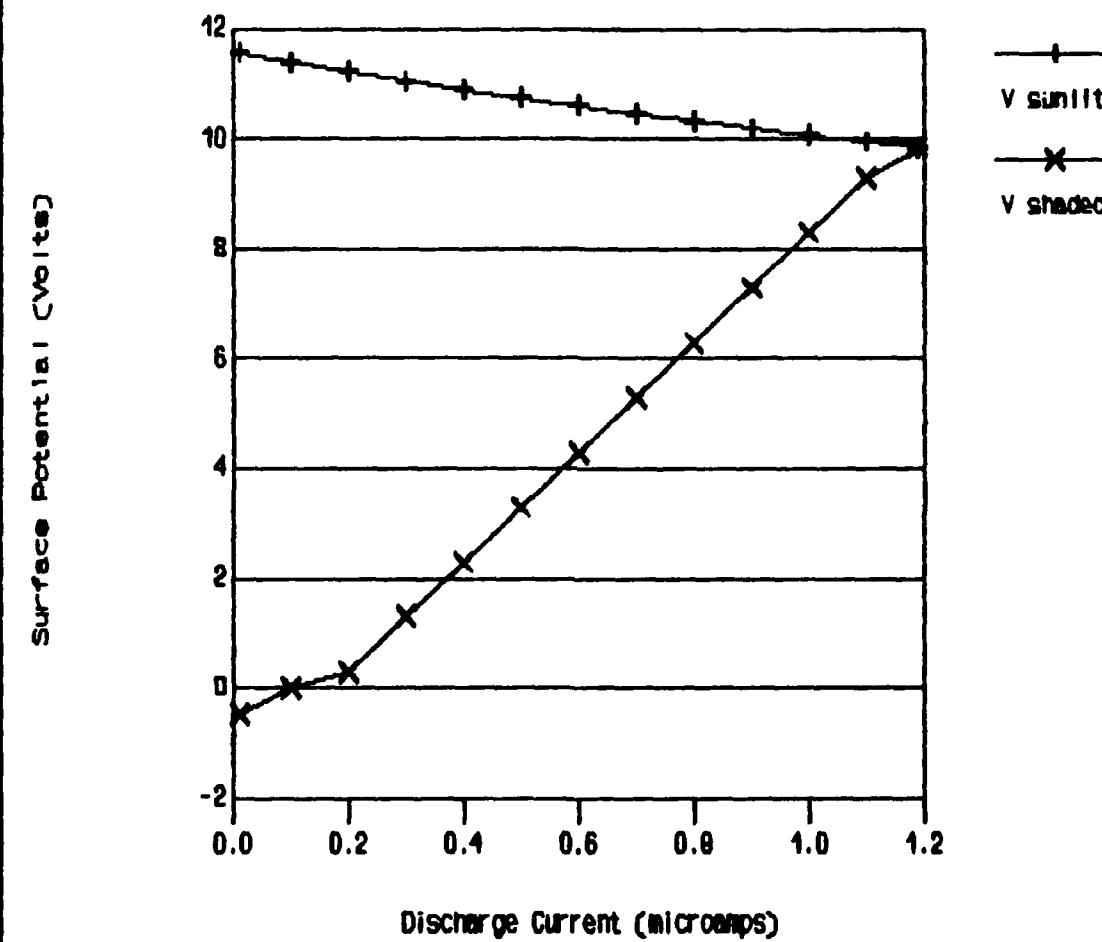


Fig 6.9 Surface Potentials in Average Plasma - No Rotation

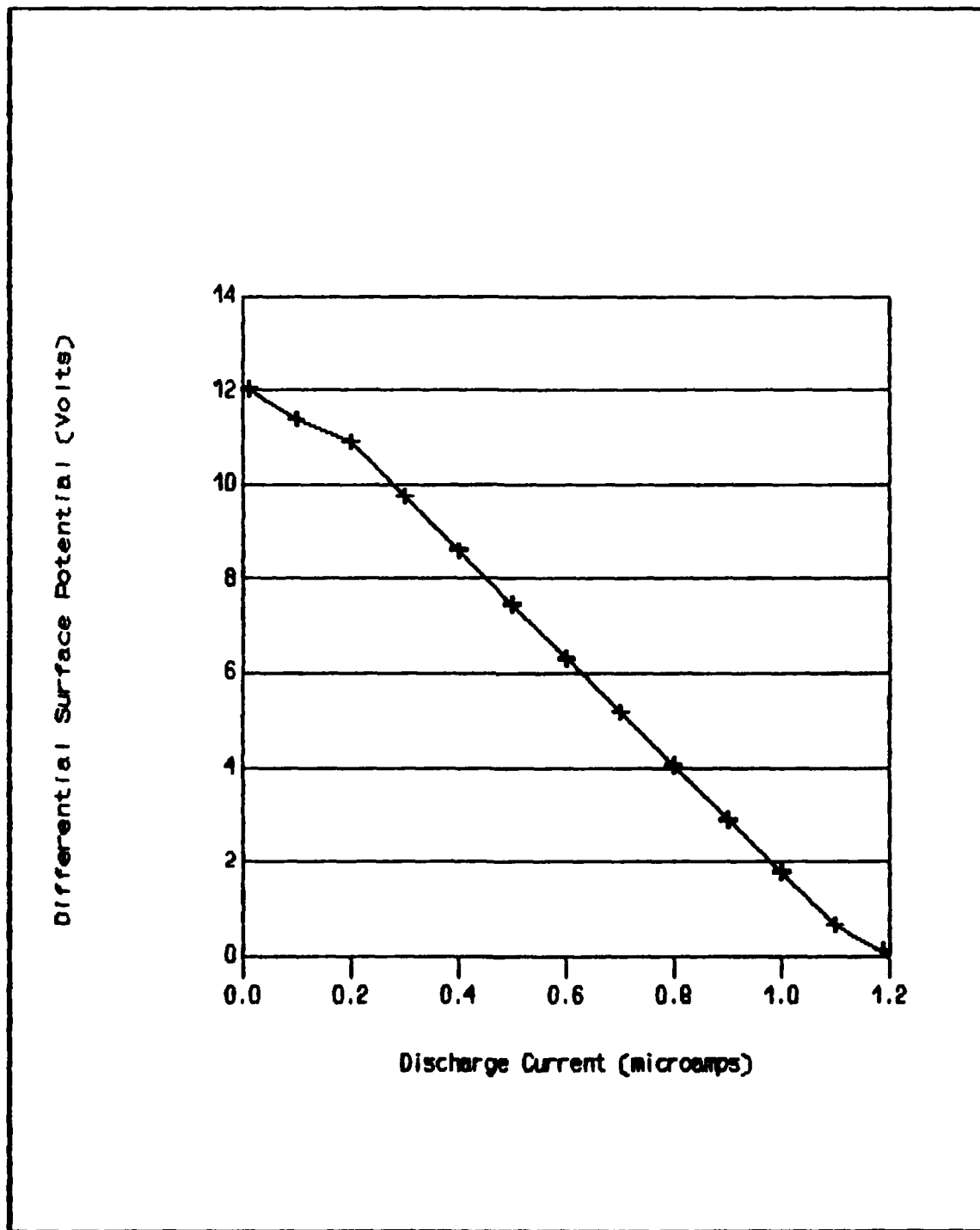


Fig 6.18 Differential Surface Potential in Average Plasma -  
No Rotation

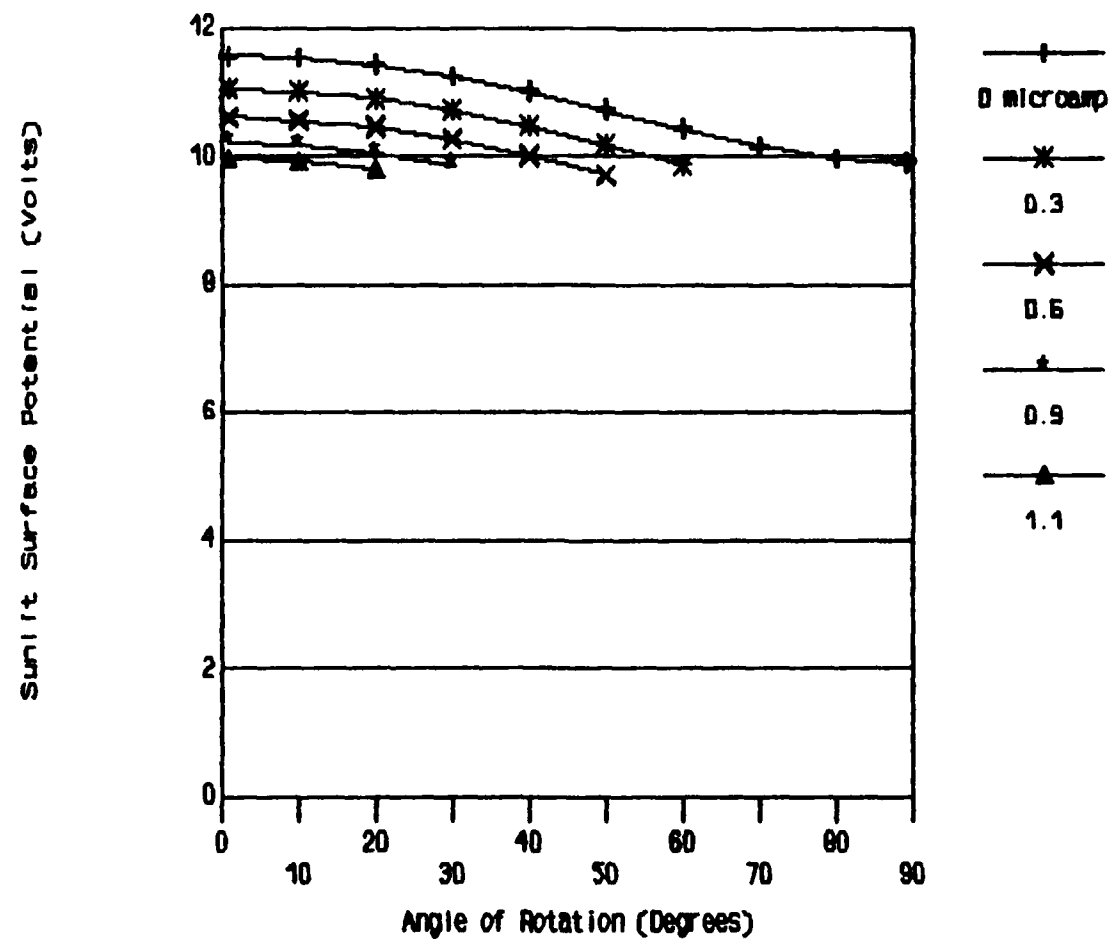


Fig 6.11 Sunlit Surface Potential in Average Plasma for Rotating Spacecraft

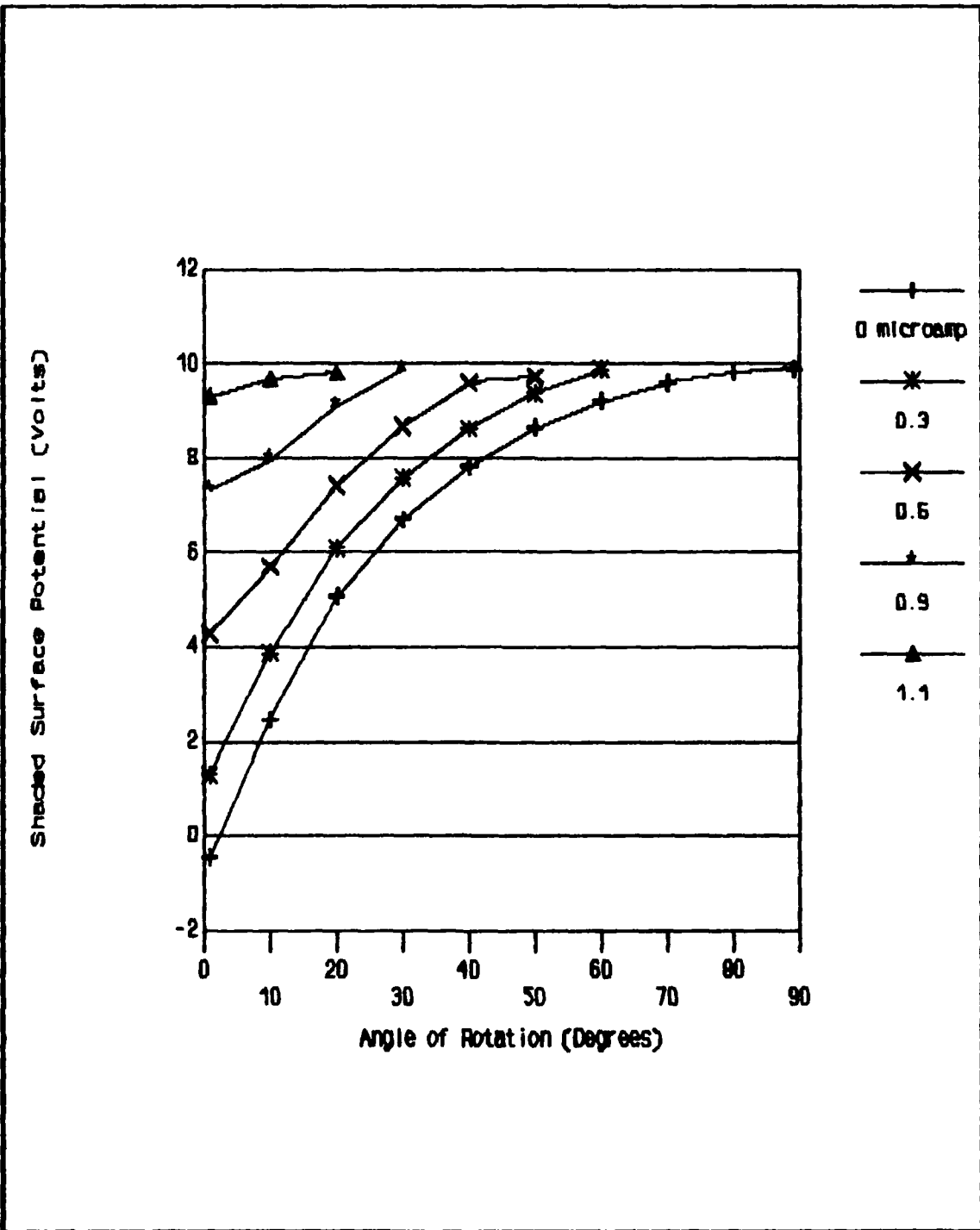


Fig 6.12 Shaded Surface Potential in Average Plasma for Rotating Spacecraft

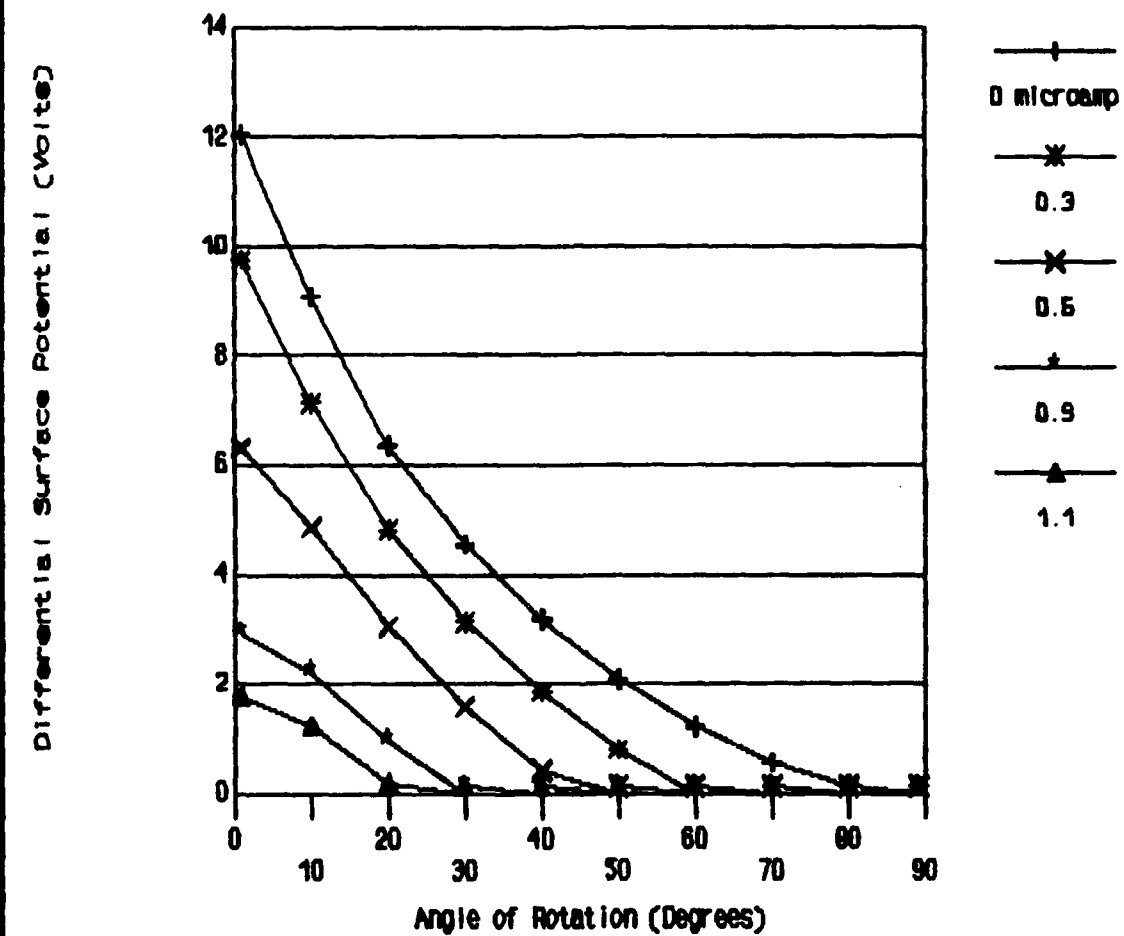


Fig 6.13 Shaded Surface Potential in Average Plasma for Rotating Spacecraft

The rotating spacecraft case shows the same dominance of photoelectron current as the shaded side is more exposed to the sun. At about 30 degrees of rotation the differential potential is about 1/3 of the initial value. Once again the maximum discharge current occurs when the surfaces are stabilized with one side totally exposed to the sun and the other side shaded.

#### Eclipse Charging

During eclipse the plasma conditions are the same at each surface of the spacecraft and no surfaces are exposed to sunlight. Calculations with the model give about -23,670 volts for both surfaces in the worst case plasma, and -0.47 volts for the average plasma case. No discharge current can occur in this case because there is no differential surface potential.

The spacecraft structural model used here has conductive surface material structure so the surface charges quickly. However, for an actual spacecraft the dielectric surface materials charge more slowly and large differential potentials can occur between conductors and dielectrics. This can result in arc discharge problems during the transition between sunlit and eclipse conditions. The same conditions for arcing occur when a spacecraft rotates in the

worst case plasma. These arc discharge problems are not of concern in this analysis, but they are significant in a real spacecraft.

#### Spacecraft Charge as a Power Source

This section discusses the suitability of spacecraft surface charge as a source of power. The power available is limited so it is compared here to the power requirements of a small electronic calculator. A comparison is also made with the power collected by a solar cell.

Worst case plasma conditions result in surface charging that can support about  $7 \times 10^{-6}$  amps at a potential of 1000 volts (Fig 6.2). Average plasma conditions can provide about  $0.6 \times 10^{-6}$  amps at 6 Volts (Fig 6.9). The approximate power available is as follows:

- a.  $1000 \times 7 \times 10^{-6} = 7 \times 10^{-3}$  Watts in worst case plasma.
- b.  $6 \times 0.6 \times 10^{-6} = 3.6 \times 10^{-6}$  Watts in average plasma.

Considering a simplified geosynchronous orbit in which worst case plasma conditions occur from midnight to dawn local time (6 hours). During eclipse (about 1 hour in worst case plasma conditions) absolute charging occurs and no

discharge current is available. The remainder of the orbit has average plasma conditions. Therefore, more than 99% of the total power available in an orbit comes from worst case plasma conditions.

Typically a small LCD (liquid crystal display) personal hand held calculator requires about  $10^{-3}$  watts of power and uses 3 Volt batteries. This means that the calculator requires about  $10^{-3}/3 = 333 \times 10^{-6}$  amps of current. Therefore, there is insufficient current available from spacecraft surface charge (one metre radius) to operate a small electronic calculator. However, the current available does scale up in proportion to the surface area exposed of the sunlit side of the spacecraft. Fig 6.14 shows the maximum expected discharge current to be about  $16 \times 10^{-6}$  amps for a spacecraft with twice the surface area. But, the spacecraft surface area required to produce sufficient current to operate the calculator is about  $48 \text{ m}^2$ . This area is large for the limited energy return expected.

Assuming a solar cell receives about  $10^3$  Watts/ $\text{m}^2$  from the sun and collects energy with 10% efficiency. The surface area required to produce  $7 \times 10^{-3}$  Watts is about  $0.07 \times 10^{-3} \text{ m}^2$ . The surface area of the spacecraft necessary to produce this same amount of power with

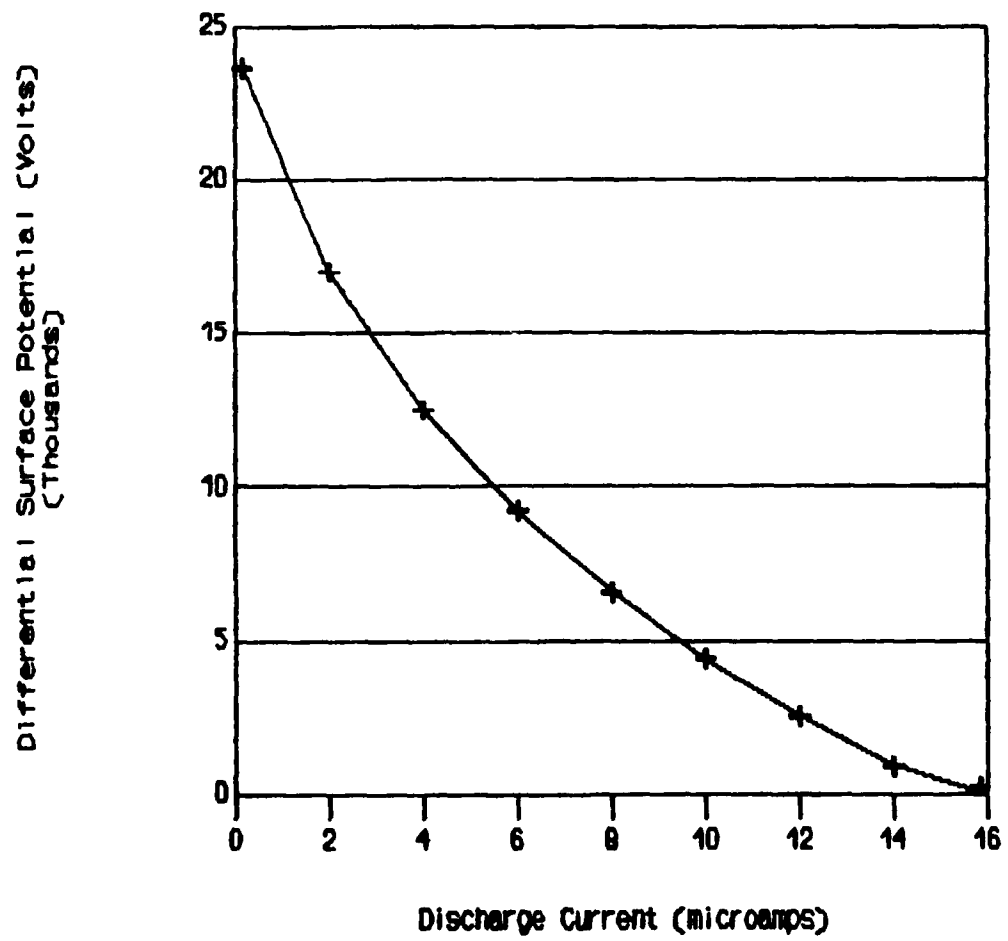


Fig 6.14 Differential Surface Potential in Worst Case Plasma - No Rotation (2 times surface area)

spacecraft charge is about  $3.14 \text{ m}^2$ . Therefore, the efficiency of spacecraft charge collection compared to a solar cell in terms of area required is 0.002%.

Table 6.1 shows that the maximum plasma particle current expected from a worst case plasma is  $82.3 \times 10^{-6}$  amps. The maximum current computed by the simulation is an order of magnitude less than this value. However, 82.3 microamps is still a small current and would be inadequate as a source of power. Particularly when this current is only possible during the short lifetime of the volatile worst case plasma environment.

## VII. CONCLUSIONS

The purpose of this thesis was to examine spacecraft charging as a possible source of electrical power for spacecraft. An analytical particle current model was used to determine spacecraft surface potentials developed in worst case and average geosynchronous plasma conditions. A discharge current between differentially charged surfaces was simulated to examine the current required to balance the surface potentials. This current approximates the maximum current that can be drawn from the spacecraft charging process.

A first-order approximation of the discharge current available from a one metre radius satellite has shown that large potential differences occur, but there is insufficient current to directly power a small hand held electronic calculator. However, the discharge current scales up with the surface area exposed and, for large spacecraft structures in the future, more usable currents may be available. But, when compared to a solar cell on the basis of the power produced per unit area, a spacecraft charge collector is four orders of magnitude less efficient.

### Limitations

This research has identified the following limitations or problems with this analysis and the implementation of a spacecraft charge collector:

- a. A worst case plasma is required to produce significant discharge currents, and this environment may only occur for up to 6 hours in an orbit.
- b. Shaded surface potentials can be large but they are sensitive to discharge current changes as small as one microamp. Electronic control circuitry would be required to limit the current drawn from the surface.
- c. The maximum surface current occurs when surfaces are either totally exposed or shaded from sunlight. Partial exposure to sunlight can suppress the negative surface potentials.
- d. Many spacecraft surface materials are dielectrics and will not conduct electric charge readily; therefore, this charging analysis does not hold for these surfaces.

e. The effects of absolute negative charging of a sunlit spacecraft could not be examined using this model. NASCAP would be suitable to complete this analysis.

The model used here has given order of magnitude approximations of the current available from spacecraft charging. A numerical three dimensional model could be used to examine the problem in more depth. However, this work has given a reasonable insight into the spacecraft charging and the energy available.

Spacecraft charge collection appears to have limited use considering the different spacecraft surface materials in use, and the problems involved in obtaining continuous conductive surfaces. Future development in conductive surface coatings and larger space structures may produce surfaces suitable to include some current collection device. However, the energy available from surface charging is small and continued materials development to eliminate charging appears to be the logical solution to spacecraft charging.

Appendix : MATHCAD 2.0 Document for Solving  
Spacecraft Charging Equations

-----  
SPACECRAFT CHARGING CURRENT BALANCE EQUATION  
TO FIND THE POTENTIALS ON A SPACECRAFT SURFACE  
-----

SPECIFY  
PLASMA CHARACTERISTICS - WORST CASE

Electrons

$$N_e := 1.12 \cdot 10^6 \text{ particle density } / \text{m}^3$$
$$T_e := 1.2 \cdot 10^4 \text{ particle temp. eV}$$

Ion

$$N_p := 0.236 \cdot 10^6 \text{ particle density } / \text{m}^3$$
$$T_i := 2.95 \cdot 10^4 \text{ particle temp. eV}$$

CONSTANTS

$$K := 1.38 \cdot 10^{-23} \text{ Boltzmann Constant}$$
$$q := 1.6 \cdot 10^{-19} \text{ electron charge}$$
$$M_e := 9.11 \cdot 10^{-31} \text{ mass of electron}$$
$$M_p := 1.67 \cdot 10^{-27} \text{ mass of proton}$$

FOR SPHERICAL SPACECRAFT

Electron Current Density in plasma - no surface potential

$$J_{eo} := \left[ q \cdot \frac{N_e}{2} \right] \cdot \left[ \frac{2 \cdot T_e \cdot q}{\pi \cdot M_e} \right]^{.5}$$

Ion Current Density in plasma - no surface potential

$$J_{io} := \left[ q \cdot \frac{N_p}{2} \right] \cdot \left[ \frac{2 \cdot T_i \cdot q}{\pi \cdot M_p} \right]^{.5}$$

## SATELLITE PARAMETERS

---

$R_{sat} := 1$  satellite radius  
metres

$A := 2 \cdot \pi \cdot R_{sat}^2$  surface area of hemisphere

$A_{eff} := \pi \cdot R_{sat}^2$  effective surface of irradiated  
surface of sphere

$J_{pho} := 20 \cdot 10^{-6}$  photoelectron emission density  
for Aluminium surface material

## SECONDARY EMISSION & BACKSCATTER PARAMETERS FOR ALUMINIUM SURFACE

---

$S_e := 0.4$  secondary electron emission  
- due to electron flux

$S_i := 3$  secondary electron emission  
- due to ion flux

$B_{Se} := 0.2$  backscatter of electrons

## INTERMEDIATE COMPUTATION CONSTANTS

---

$I_e := J_{eo} \cdot A$  plasma electron current

$I_i := J_{io} \cdot A$  plasma ion current

$I_{ph} := J_{pho} \cdot A_{eff}$  photoelectron current

$X := \frac{q}{K \cdot T}$  for T in degrees K  
but will use  $X_e$ ,  $X_i$  and  $X_{ph}$   
below for T in eV

$X_e := \frac{1}{T_e}$  constant - for electrons

$X_i := \frac{1}{T_i}$  constant - for ions

$X_{ph} := \frac{1}{3}$  approximate factor for  
photoelectrons (Garrett, 1981:611)

---

**EQUATIONS FOR CURRENT FLOW BETWEEN CHARGED SURFACES  
OF THE SPACECRAFT**

---

$V_1$  = potential of photoelectron dominated side  
 $V_2$  = potential of plasma current dominated side  
 $F_1$  = fraction of side 1 irradiated  
 $1-F_1$  = fraction of side 2 irradiated

$I_t := 0$  surface discharge current  
 $C_e := 1 - S_e - B S_e$  fraction of electrons incident  
 $C_i := 1 + S_i$  fraction of ions incident

**EQUATIONS ARE SOLVED FOR SURFACE POTENTIALS  
 $V_1$  AND  $V_2$**

**FOR:  $V_1$  (+)VE,  $V_2$  (-)VE**

---

Guess  $V_1 := 10$  initial potential values  
 $V_2 := -10$  for iteration

**GIVEN**

$$I_e \cdot (1 + X_e \cdot V_1) - I_i \cdot e - F_1 \cdot I_{ph} \cdot e + I_t \approx 0$$

$$I_e \cdot C_e \cdot e - I_i \cdot C_i \cdot (1 - X_i \cdot V_2) - (1 - F_1) \cdot I_{ph} - I_t \approx 0$$

**SURFACE POTENTIALS  
FUNCTION DEFINITION #1**

$C_1(I_t, F_1) := \text{find}(V_1, V_2)$

$C_1(I_t, F_1) = 0$

$C_1(I_t, F_1) = 1$

**REDEFINE POTENTIAL FOR  $V_2$**

**FOR:  $V_1$  (+)VE,  $V_2$  (+)VE - WITH  $V_2 < V_1$**

---

**Guess  $V_2 := 10$**

**GIVEN**

$$I_e \cdot (1 + X_e \cdot V_2) - I_i \cdot e - (1 - F_1) \cdot I_{ph} \cdot e - I_t \approx 0$$

**SURFACE POTENTIALS  
FUNCTION DEFINITION #2  
POTENTIAL  $V_2$**

-----  
SOLVE FOR SURFACE POTENTIALS V1 AND V2  
FOR A RANGE OF ROTATION ANGLES  $\theta$  AND  
SURFACE DISCHARGE CURRENTS  $I_t$   
-----

DEFINE VARIABLES TO CHANGE DURING SPACECRAFT ROTATION

$$\theta := \frac{\pi}{9}, \frac{\pi}{18}, \dots, \frac{\pi}{2}$$

rotation angle of spacecraft  
symmetrical for sphere

$$F1(\theta) := \frac{1}{2} + \frac{\left[ \sin \left[ \frac{\pi}{2} - \theta \right] \right]^2}{2}$$

surface area illuminated for  
side 1 of sphere rotated by  
angle  $\theta$  up to 180 deg

$$1 - F1(\theta) =$$

surface area illuminated for  
side 2 of sphere rotated by  
angle  $\theta$  up to 180 deg

$\theta = 90$  degrees computed since symmetry exists for  
a spherical spacecraft

Define discharge current Range  $I_t$

$$I_t := 0, 1 \cdot 10^{-6} \dots 9 \cdot 10^{-6}$$

SOLVE AND WRITE DATA FILES TO DISK

-----

WRITERPN(R1) := C1(I<sub>t</sub>, F1( $\theta$ ))  
     $\theta$

WRITERPN(R2) := A1(I<sub>t</sub>, F1( $\theta$ ))  
    1

WRITERPN(R3) := C2(I<sub>t</sub>, F1( $\theta$ ))

DATA IS REORGANIZED AND PLOTTED USING  
A SPREADSHEET

TO SOLVE FOR AVERAGE PLASMA NEED TO CHANGE  
DECLARED PLASMA VARIABLES AND RECOMPUTE.  
THE RANGES OF DISCHARGE CURRENTS CAN BE  
CHANGED BY ENTERING NEW RANGE VARIABLE  
VALUES IN THE  $I_t$  DECLARATION

## BIBLIOGRAPHY

Bass, J.N. and others. Analysis of Geophysical Data-Bases and Models for Spacecraft Interactions: Final Technical Report. August 1983 - October 1986. Contract F19628-83-C0105. Carlisle: RADEX Inc, 31 October 1986. (AFGL-TR-86-0221), (AD-A184809).

Cassidy, J.J. NASCAP User's Manual. 1978. (NASA-CR-159417).

Chapman, Brian. Glow Discharge Processes. New York: John Wiley and Sons, 1980.

Chen, Francis F. Introduction to Plasma Physics. New York: Plenum Press, 1974.

Garrett, H.B. "Modeling of the Geosynchronous Plasma Environment," Spacecraft Charging Technology - 1978, 11-22. (NASA-CP-2071), (AFGL-TR-79-0082).

Garrett, H.B. "The Charging of Spacecraft Surfaces," Review of Geophysics and Space Physics, 19: 577-616 (November 1981).

Higgins, Daniel F. "An Analytical Model of Multi-Dimensional Spacecraft Charging Fields and Potentials," IEEE transactions on Nuclear Sciences, 26: 5162-5167 (December 1979).

Katz, I. and others. "Secondary Electron Generation, Emission and Transport: Effects on Spacecraft Charging and NASCAP Models," The Aerospace Environment at High Altitudes and its Implications for Spacecraft Charging and Communications, 1-12, May 1987. (AGARD-CP-406).

Katz, I. and others. "The Capabilities of the NASA Charging Analyzer Program," Spacecraft Charging Technology - 1978, 101-122. (NASA-CP-2071), (AFGL-TR-79-0082).

Katz, I. and others. "Dynamic Modeling of Spacecraft in a Collisionless Plasma," Proceedings of the Spacecraft Technology Conference, 319-330, February 1977. (NASA-TMX-73537), (AFGL-TR-77-0051), (AD-A045459).

Laframboise, J.G. and others. "Results from a Two-Dimensional Spacecraft-Charging Simulation and Comparison with a Surface Photocurrent Model," Spacecraft Charging Technology - 1980. 708-716. (NASA-CP-2182), (AFGL-TR-81-0270).

Lovell, Robert R. and others. "Spacecraft Charging Investigation: A Joint Research and Technology Program," Progress in Astronautics and Aeronautics, 47: Spacecraft Charging by Magnetospheric Plasmas: 3-14, 1976.

Massaro, M.J. and others. "A Charging Model for Three-Axis Stabilized Spacecraft," Proceedings of the Spacecraft Technology Conference. 237-269, February 1977. (NASA-TMX-73537), (AFGL-TR-77-0051), (AD-A045459).

McPherson, D.A. and W.R. Schrober. "Spacecraft Charging at High Altitudes," Progress in Astronautics and Aeronautics, 47: Spacecraft Charging by Magnetospheric Plasmas: 15-30, 1976.

Nicholson, Dwight R. Introduction to Plasma Theory. New York: John Wiley and Sons, 1983.

O'Donnell, E.E. "Spacecraft Charge Modeling Development and Validation Study," Spacecraft Charging Technology - 1978. 797-816. (NASA-CP-2071), (AFGL-TR-79-0082).

Purvis, Carolyn K. and others. Design Guidelines for Assessing and Controlling Spacecraft Charging Effects. September 1984. (NASA-TP-2361).

Sanders, N.L. and G.T. Inouye. "NASCAP Charging Calculations for a Synchronous Orbit Satellite," Spacecraft Charging Technology - 1980. 684-708. (NASA-CP-2182), (AFGL-TR-81-0270).

Stannard, P.R. and others. "Validation of the NASCAP Model Using Spaceflight Data," AIAA 20th Aerospace Sciences Meeting. 1-12, 11 January - 14 January 1982. (AIAA-82-0269).

Stettner, R. and others. "Physical Modeling of Spacecraft Discharge Processes and Associated Electron Blowoff," IEEE Transactions on Nuclear Science. 27: 1780-1785 (December 1980).

Stevens, John N. and others. "Modeling of Environmentally Induced Transients Within Satellites," Journal of Spacecraft and Rockets, 24: 257-263 (May 1987).

Tamm, I.E. Fundamentals of the Theory of Electricity. Moscow: Mir Publishers, 1979.

Whipple, Elden C. Jr. "Modeling of Spacecraft Charging," Proceedings of the Spacecraft Charging Technology Conference. 225-235, February 1977. (NASA-TMX-73537), (AFGL-TR-77-0051), (AD-A045459).

VITA

Wayne Gale [REDACTED]

[REDACTED] He joined the Royal Australian Air Force (RAAF) in 1971 and graduated as an Instrument Fitter in 1973. He worked on general aircraft instrumentation, and also Mirage aircraft flight controls and navigation systems for five years. In 1979 he started studying at the Royal Melbourne Institute of Technology, Melbourne, Australia, and received the degree of Bachelor of Engineering in Electronic Engineering in May 1983. He received a commission in the RAAF and was employed as Officer in Charge of ground radio, radar, and navigation equipment maintenance at RAAF Base Williamtown, NSW. Following this he was employed at RAAF Headquarters Support Command, Melbourne, Australia, as the systems engineer responsible for installation of computers, data communications, and microwave radio link equipment. He entered the School of Engineering, Air Force Institute of Technology, in May 1987.

Permanent Address: [REDACTED]

## UNCLASSIFIED

SECURITY CLASSIFICATION OF THIS PAGE

DRAFT. Do not use

## REPORT DOCUMENTATION PAGE

Form Approved  
OMB No. 0704-0188

|   |  |  |                                       |
|---|--|--|---------------------------------------|
| 1a REPORT SECURITY CLASSIFICATION<br><b>UNCLASSIFIED</b>  |  | 1b RESTRICTIVE MARKINGS  |                                       |
| 2a SECURITY CLASSIFICATION AUTHORITY  |  | 3 DISTRIBUTION/AVAILABILITY OF REPORT<br><b>Approved for public release;<br/>distribution unlimited.</b>   |                                       |
| 2b DECLASSIFICATION/DOWNGRADING SCHEDULE  |  |  |                                       |
| 4 PERFORMING ORGANIZATION REPORT NUMBER(S)<br><b>AFIT/GSO/ENP '88D-2</b>  |  | 5 MONITORING ORGANIZATION REPORT NUMBER(S)   |                                       |
| 6a NAME OF PERFORMING ORGANIZATION<br><b>School of Engineering</b>  | 6b OFFICE SYMBOL<br>(If applicable)<br><b>AFIT/ENS</b> | 7a. NAME OF MONITORING ORGANIZATION  |                                       |
| 6c. ADDRESS (City, State, and ZIP Code)<br><b>Air Force Institute of Technology (AU)<br/>Wright-Patterson AFB, OH 45433-6583</b>  |  | 7b ADDRESS (City, State, and ZIP Code)   |                                       |
| 8a. NAME OF FUNDING/SPONSORING<br>ORGANIZATION  | 8b OFFICE SYMBOL<br>(If applicable)                    | 9 PROCUREMENT INSTRUMENT IDENTIFICATION NUMBER   |                                       |
| 8c. ADDRESS (City, State, and ZIP Code)   |  | 10 SOURCE OF FUNDING NUMBERS   |                                       |
|   |  | PROGRAM<br>ELEMENT NO  | PROJECT<br>NO                         |
|   |  | TASK<br>NO   | WORK UNIT<br>ACCESSION NO             |
| 11. TITLE (Include Security Classification)<br><b>See Box 19</b>  |  |  |                                       |
| 12 PERSONAL AUTHOR(S)<br><b>Wayne Gale, B.E., FLTLT, RAAF</b>   |  |  |                                       |
| 13a TYPE OF REPORT<br><b>MS Thesis</b>  | 13b TIME COVERED<br>FROM _____ TO _____                | 14. DATE OF REPORT (Year, Month, Day)<br><b>1988 November</b>  | 15. PAGE COUNT<br><b>107</b>          |
| 16. SUPPLEMENTARY NOTATION  |  |  |                                       |
| 17. COSATI CODES  |  | 18. SUBJECT TERMS (Continue on reverse if necessary and identify by block number)<br><b>Spacecraft, Electric Power Production</b><br><b>Space Charge, Electrostatic Charge</b> |                                       |
| 19. ABSTRACT (Continue on reverse if necessary and identify by block number)  |  |  |                                       |
| <p><b>Title: SPACECRAFT CHARGE AS A SOURCE OF<br/>ELECTRICAL POWER FOR SPACECRAFT</b></p> <p><b>Thesis Advisor: Howard E. Evans, Lt. Col., USAF<br/>Instructor of Physics</b></p> <p><i>Approved for release in<br/>accordance with AFR 190-1<br/>12 Jan 1987</i></p> |  |  |                                       |
| 20 DISTRIBUTION/AVAILABILITY OF ABSTRACT<br><input checked="" type="checkbox"/> UNCLASSIFIED/UNLIMITED <input type="checkbox"/> SAME AS RPT <input type="checkbox"/> DTIC USERS   |  | 21. ABSTRACT SECURITY CLASSIFICATION<br><b>UNCLASSIFIED</b>  |                                       |
| 22a. NAME OF RESPONSIBLE INDIVIDUAL<br><b>Howard E. Evans, Lt. Col., USAF</b>   |  | 22b TELEPHONE (Include Area Code)<br><b>(513) 255 2012</b>   | 22c. OFFICE SYMBOL<br><b>AFIT/ENP</b> |

This thesis examines the suitability of spacecraft charge, collected at geosynchronous altitude, as a source of electrical power for spacecraft. An analytical plasma probe model is used to describe the flux of charged particle currents on two isolated (conductive) hemispheres of a spacecraft. Surface potentials are evaluated for both a body-stabilized and spin-stabilized spacecraft under average and worst case plasma conditions. A discharge current is simulated, between differentially charged surfaces, to examine the current flow required to balance the surface potentials. This current approximates the maximum current flow available from the spacecraft charge. The results show that surface potential differences can be large in worst case plasma conditions, but the current available is too small to be useful as a power source. The discharge current does scale up in proportion to spacecraft surface area exposed to the plasma; however, the design of large conductive spacecraft surfaces is a problem in itself.